Articles

Independent Synthesis, Solution Behavior, and Studies on the Mechanism of Formation of a Primary Amine-Derived Fluorophore Representing Cross-linking of Proteins by (*E*)-4-Hydroxy-2-nonenal

Guozhang Xu, Yahua Liu, and Lawrence M. Sayre*

Department of Chemistry, Case Western Reserve University, Cleveland Ohio 44106

Received December 29, 1998

Lipid peroxidation in aging and degenerative disease results in the production of 4-hydroxy-2-alkenals that modify proteins and give rise to both protein cross-linking and fluorophore generation. Recent model studies demonstrated that the major ex/em 360/430 fluorophore formed from (*E*)-4-hydroxy-2-nonenal (HNE) or (*E*)-4-hydroxy-2-hexenal (HHE) and protein lysine-based amine is a 2-alkyl-2-hydroxy-1,2-dihydropyrrol-3-one iminium 1:2 cross-link (**1**), a structure that is further confirmed here using ^{15}N-labeling, and which has pH stability characteristics the same as those of lipofuscin pigments isolated from human tissues. Fluorophore generation represents an overall four-electron oxidation, requires dioxygen, and is enhanced by the presence of Cu(II). The HNE−propylamine-derived fluorophore **1a** was independently synthesized from either 3,4-dioxononanal (**8**) or (*E*)-4-oxo-2-nonenal (**13**), providing further evidence for its assigned structure and clues to how it forms from HNE. Mechanistic studies on HNE-derived fluorophore formation permit ruling out the initial reversible HNE-derived Schiff base Michael adduct (**17**) as an intermediate. In addition, the structurally related non-cross-link 2-pentyl-2-hydroxy-1,2-dihydropyrrol-3-one **9a** that forms along with **1a** from **8** does not form from HNE and does not serve as a precursor to **1a** in the HNE−amine reaction system. A mechanism involving two 2e oxidations following initial Schiff base formation is proposed that is consistent with intermediates independently accessed from **8** and **13**.

Introduction

An accumulation of fluorescent pigments, lipofuscin and ceroid, is one of the most frequently observed cytologic changes associated with age in postmitotic cells and/or with certain pathological degenerative processes.[1,2] It is generally believed that the fluorescent pigments are end-products of free radical induced lipid peroxidation of subcellular components.[3−5] The fluorescent pigments formed from lipid peroxidation have emission maxima in the region of 430−470 nm when excited at 360−390 nm.[6] Because of the high sensitivity, this fluorescence is widely used as a parameter for assessing oxidative damage in biological systems,[6−8] ascribed to reaction of diffusible lipid-derived reactive aldehydes such as (*E*)-4-hydroxy-2-nonenal (HNE), (*E*)-4-hydroxy-2-hexenal (HHE), malondialdehyde (MDA), and 2-alkenals with proteins and aminophospholipids.[9−15] In early studies, Chio and Tappel[11,12] suggested that fluorescent products derived from the reaction of MDA with amino acids were conjugated Schiff bases with the general structure RNHCH═CHCH═NR (*N*,*N*′-disubstituted 1-amino-3-iminopropenes), which exhibited ∼390/470 nm (ex/em) fluorescence. Kikugawa et al.[14,15] later proposed 1,4-dihydropyridine-3,5-dicarboxaldehydes to be the major lipofuscin-like fluorophores (ex/em ∼400/460) generated in the reaction of primary amines with MDA. However, these fluorescence characteristics are quite different from those observed in lipid extracts of oxidatively damaged cellular organelles.[3,4] This suggests that MDA, which has been considered a precursor of fluorescent substances, is of lesser significance in the formation of lipofuscin-like fluorescent substances.

* To whom correspondence should be addressed. E-mail: lms3@po.cwru.edu.

(1) Shimasaki, H.; Maeba, R.; and Ueta, N. In *Lipofuscin and Ceroid Pigments*; Porta, E. A., Ed.; Plenum Press: New York. 1990; pp 323−331.
(2) Yin, D. *Free Radical Biol. Med.* **1996**, *21*, 871−888.
(3) Kikugawa, K.; Beppu, M. *Chem. Phys. Lipids* **1987**, *44*, 277−296.
(4) Tsuchida, M.; Miura, T.; Aibara, K. *Chem. Phys. Lipids* **1987**, *44*, 297−325.
(5) Fletcher, B. L.; Dillard, C. J.; Tappel, A. L. *Anal. Biochem.* **1973**, *52*, 1−9.
(6) Taubold, R. D. *Lipids* **1975**, *10*, 383−390.
(7) Shimasaki, H.; Ueta, N.; Privett, O. S. *Lipids* **1982**, *17*, 878−883.
(8) Tsuchida, M.; Miura, T.; Mizutani, K.; Albara, K. *Biochim. Biophys. Acta* **1985**, *834*, 196−204.
(9) Esterbauer, H.; Schaur, R. J.; Zollner, H. *Free Radical Biol. Med.* **1991**, *11*, 81−128.
(10) Nair, V.; Offerman, R. J.; Turner, G. A.; Pryor, A. N.; Baenziger, N. C. *Tetrahedron* **1988**, *44*, 2793−2803.
(11) Chio, K. S.; Tappel, A. L. *Biochemistry* **1969**, *8*, 2821−2827.
(12) Chio, K. S.; Tappel, A. L. *Biochemistry* **1969**, *8*, 2827−2833.
(13) Alaiz, M.; Barragan, S. *Chem. Phys. Lipids* **1995**, *77*, 217−223.
(14) Kikugawa, K.; Iwata, A.; Beppu, M. *Chem. Pharm. Bull.* **1988**, *36*, 685−692.
(15) Kikugawa, K.; Ido, Y. *Lipids* **1984**, *19*, 600−608.

10.1021/jo982523j CCC: $18.00
Published on Web 07/20/1999

Lipoxidation-derived 4-hydroxy-2-alkenals,[9,16] especially HNE and HHE, are highly toxic, react readily with proteins and aminophospholipids under physiological conditions, and have been implicated in various neurodegenerative diseases[17−19] and in the oxidative damage to low-density lipoprotein (LDL) that underlies the initial stages of atherosclerosis.[20−22] There is increasing evidence that these aldehydes are the major contributors to the ex/em 360/430 nm fluorescence seen in oxidatively damaged LDL (oxLDL) as well as in the poorly defined ceroid pigments associated with atherosclerotic plaques.[23−26] The contribution of HNE or HHE to this fluorescence was demonstrated in recent work on the isolation[27−29] and structural characterization[27,28] of one major ex/em 360/430 nm fluorophore that arises from *cross-linking* of two primary amines by one 4-hydroxy-2-alkenal and for which there is immunochemical evidence for its formation on proteins.[29] We assigned 2-alkyl-2-hydroxy-1,2-dihydropyrrol-3-one iminium (**1**) to the structure of the fluorophore,[27] and further evidence supporting our assignment is provided in this study. We also report characteristics of this HNE- or HHE-derived fluorophore that are consistent with it being a major contributor to age-related fluorescent substances (ARFS).[1,3,4] We further find that the formation rate and ultimate yield of the ex/em 360/430 nm fluorescence is enhanced in parallel to the level of HNE-derived protein cross-linking by the presence of Cu(II), a transition metal often used to initiate lipid peroxidation in vitro.[30] A better understanding of the mechanism of formation of the ex/em 360/430 nm fluorophore from 4-hydroxy-2-alkenals revealed in the present studies may shed new light on the physiological accumulation of lipoxidation-dependent protein-based fluorophores during aging and degenerative disease.

Results and Discussion

1. Fluorophore Formation in Reactions of Primary Amines with HNE or HHE. The long-standing interest of this laboratory in lipoxidation-dependent protein cross-linking in aging and degenerative disease initiated our recent work on the isolation of a fluorophore from model reactions of HNE or HHE with primary amines (e.g., *n*-butylamine or *n*-propylamine) that serve as mimics of protein lysine side chains. These reactions were previously observed to result in complex substance profiles (e.g., as viewed by TLC[31]). More recent analysis by HPLC revealed that a very characteristic fluorophore with ex/em 360/430 nm was formed in these reactions, though in low yield.

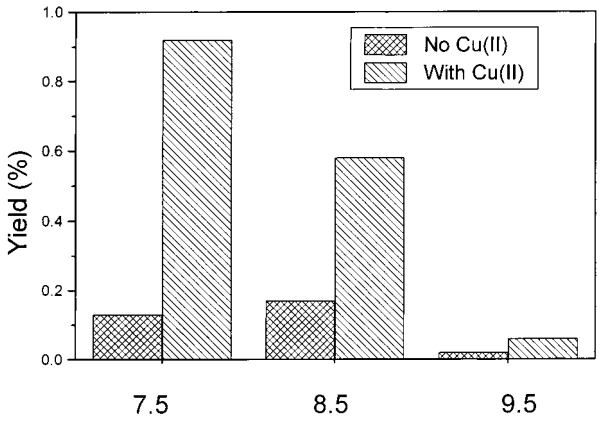

Figure 1. Effect of pH on fluorophore **1b** formation in the reaction of HNE (80 mM) with *n*-butylamine (320 mM) in the presence and absence of (2,2′-bipyridine)$_2$Cu(II) (0.4 mM).

To facilitate isolation and characterization of this fluorophore, we conducted a series of experiments by varying the pH, the ratio of HNE or HHE to *n*-butylamine, the reaction time, and the presence or absence of Cu(II). These results indicated that optimal fluorophore formation required an excess of *n*-butylamine to HNE or HHE (∼5−10:1) and neutral to slightly basic pH. At pH < 7, the rate of fluorophore development was impractically slow, presumably because of the absence of free base amine, though increasing the pH above 7.5 also results in decreasing yields (Figure 1), a result consistent with our finding of base instability of the fluorophore (vide infra). In addition, fluorophore formation strictly required dioxygen (no fluorescence appeared under argon) and was accelerated by Cu(II) (0.5% based on HNE or HHE) (Figure 1), consistent with the fact that the structure ultimately assigned represented a 4e oxidation stoichiometry. However, the free radical scavengers 4-*tert*-butylphenol (40 mM) and vitamin C (40 mM) exhibited only ∼10% inhibition of the generation of fluorophore from HNE and butylamine under the conditions described (with Cu^{2+}) in Figure 1 (data not shown), indicating that the reaction does not follow a radical chain mechanism. We presume that dioxygen acts as the ultimate electron acceptor for fluorophore formation in vitro and in vivo, though we have not studied the stoichiometry of dioxygen reduction.

Finally, the isolation of these fluorescent products **1** (Scheme 1) from incubation of *n*-butylamine or *n*-propylamine with HNE or HHE in pH 7.5 phosphate was achieved through repeated reversed-phase HPLC and flash chromatographic purification in 0.14−0.18% yield based on starting 4-hydroxy-2-alkenal.

2. Structural Confirmation of the HNE-Derived Fluorophore. On the basis of NMR spectroscopy (^{1}H, ^{13}C, APT, ^{1}H−^{1}H COSY) and HRMS (see the Experimen-

(16) Montine, T. J.; Amarnath, V.; Martin, M. E.; Strittmatter, W. J.; Graham, D. G. *Am. J. Pathol.* **1996**, *148*, 89−93.
(17) Sayre, L. M.; Zelasko, D. A.; Harris, P. L. R.; Salomon, R. G.; Perry, G.; Smith, M. A. *J. Neurochem.* **1997**, *68*, 2092−2097.
(18) Yoritaka, A.; Hattori, N.; Uchida, K.; Tanaka, M.; Stadtman, E. R.; Mizuno, M. *Proc. Natl. Acad. Sci. U.S.A.* **1996**, *93*, 2696−2701.
(19) Montine, K. S.; Olson, S. J.; Amarnath, V.; Whetsell, W. O., Jr.; Graham, D. G.; Montine, T. J. *Am. J. Pathol.* **1997**, *150*, 437−443.
(20) Palinski, W.; Rosenfeld, M. E.; Yla-Herttuala, S.; Gurtner, G. C.; Socher, S. S.; Butler, S. W.; Parthasarathy, S.; Carew, T. E.; Steinberg, D.; Witztum, J. L. *Proc. Natl. Acad. Sci. U.S.A.* **1989**, *86*, 1372−1376.
(21) Hoff, H. F.; O'Neil, J.; Chisolm, G. M., III.; Cole, T. B.; Quehenberger, O.; Esterbauer, H.; Jurgens, G. *Arteriosclerosis* **1989**, *9*, 538−549.
(22) Steinberg, D.; Parthasarathy, S.; Carew, T. E.; Khoo, J. C.; Witztum, J. L. *N. Engl. J. Med.* **1989**, *320*, 915−924.
(23) Esterbauer, H.; Koller, E.; Slee, R. G.; Koster, J. F. *Biochem. J.* **1986**, *239*, 405−409.
(24) Hoff, H. F.; Whitaker, T. E.; O'Neil, J. *J. Biol. Chem.* **1992**, *267*, 602−609.
(25) Steinbrecher, U. P. *J. Biol. Chem.* **1987**, *262*, 3603−3608.
(26) Esterbauer, H.; Dieber-Rotheneder, M.; Waeg, G.; Striegl, G.; Jurgens, G. *Chem. Res. Toxicol.* **1990**, *3*, 77−92.
(27) Xu, G.; Sayre, L. M. *Chem. Res. Toxicol.* **1998**, *11*, 247−251.
(28) Itakura, K.; Osawa, T.; Uchida, K. *J. Org. Chem.* **1998**, *63*, 185−187.
(29) Tsai, L.; Szweda, P. A.; Vinogradova, O.; Szweda, L. I. *Proc. Natl. Acad. Sci. U.S.A.* **1998**, *95*, 7975−7980.
(30) Jurgens, G.; Hoff, H. F.; Chisolm, G. M., III; Esterbauer, H. *Chem. Phys. Lipids* **1987**, *45*, 315−336.
(31) Sayre, L. M.; Arora, P. K.; Iyer, R. S.; Salomon, R. G. *Chem. Res. Toxicol.* **1993**, *6*, 19−22.

Scheme 1

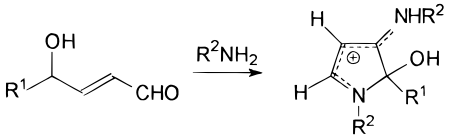

1

1a: $R^1 = C_5H_{11}$, $R^2 = C_3H_7$
1b: $R^1 = C_5H_{11}$, $R^2 = C_4H_9$
1c: $R^1 = C_2H_5$, $R^2 = C_4H_9$
1d: $R^1 = C_5H_{11}$, $R^2 = C_2H_5OCH_3$
1e: $R^1 = C_2H_5$, $R^2 = C_2H_5OCH_3$

tal Section), the structure of **1b** and **1c** was previously assigned by us to be 2-alkyl-2-hydroxy-1,2-dihydropyrrol-3-one iminium derivatives.[27] Parallel, independent work by Itakura et al.[28] led to the proposal of the analogous fluorophore formed from HNE and N^{α}-hippuryllysine, though they claimed the structure was the neutral conjugate base, a distinction that was not apparent from their NMR data. Our conclusion that fluorophore **1** exists in its resonance stabilized cationic form at neutral pH was affirmed by the finding that the ^{1}H and ^{13}C NMR spectra of compound **1** in DMSO-d_6 are unchanged upon the addition of either CF_3COOH or $NaHCO_3$. Also, the UV−vis and fluorescence spectra are unchanged from pH 1 up to the point (pH > 9) where irreversible base-induced decomposition begins to occur as evidenced by monitoring the ^{1}H NMR spectrum and fluorescence intensity following reacidification (vide infra).

For the fluorophore derived from HNE and propylamine, we initially considered on the basis of the HRMS data three other possible isomers **2**−**4** besides **1a** that were consistent with the general NMR patterns. We then excluded the α,β-unsaturated-amide and -amidine **3** and **4** on the basis that one would expect the ^{1}H NMR vinyl signals to be separated by only about 1 ppm, whereas the 2.8 ppm difference seen was more consistent with the vinylogous-amide and -amidine **2** and **1a**. Our preference for **1a** over **2** was based on the expected spin−spin coupling between the heteroatom-bound protons and the amine-based NCH_2, observable in DMSO-d_6.[27] No such distinguishing evidence was provided by Itakura et al.,[28] though they did not realize that the compound was a protonated cation.

In an effort to achieve unambiguous structural confirmation that did not rely on an argument based on spin coupling of exchangeable protons, we independently synthesized the doubly ^{15}N-labeled analogue of **1a** using [^{15}N]-propylamine. It can be seen by inspection that

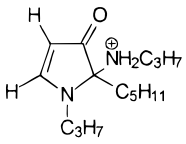

2

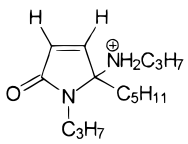

3

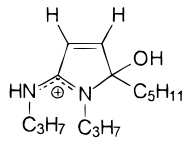

4

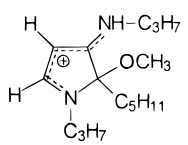

5

structures **2**−**4** all interpose only one carbon between the two nitrogens, so that one would expect to see in the proton-decoupled ^{13}C NMR spectrum three ^1J ^{13}C−^{15}N doublets and one triplet, whereas structure **1a** would exhibit five ^1J ^{13}C−^{15}N doublets. The actual spectrum clearly showed five doublets (Figure 2), including two downfield sp^2 carbon signals at 166.74 and 176.84 ppm, thereby confirming that the structure is **1a**. Consistent with the structure being **1a** rather than **2**, exposure of the adduct to methanol over silica gel resulted in its partial conversion to 2-methoxy-2-pentyl-1,2-dihydropyrrol-3-one iminium **5**. Also, typical of other cationic vinylogous amidinium compounds,[32] the 4-**H** of compound **1a** is slowly exchanged into 4-**D** in D_2O (Scheme 2).

3. Independent Synthesis of Fluorophore 1a. To provide further evidence for our assignment of structure **1** to the isolated fluorophore and to gain insight into the mechanisms of its formation and, in turn, of HNE-dependent protein cross-linking, we chose to synthesize higher oxidation state analogues of HNE that might access **1a** more efficiently. Our first strategy is outlined in Scheme 3. Metalation of 1-heptyne with *n*-butyllithium followed by reaction with bromoacetaldehyde diethyl acetal in THF at −78 °C gave 1,1-diethoxy-3-nonyne (**6**), which was then oxidized to 1,1-diethoxy-3,4-nonanedione (**7**) by ozonized oxygen.[33] Deprotection of **7** gave the desired 3,4-dioxononanal (**8**), which upon subsequent incubation with propylamine in sodium phosphate buffer (pH 4.75)/acetonitrile (3:1, v/v) gave **1a** in 25% overall yield following preparative HPLC isolation. Actually, the major product of this reaction was the 1:1 adduct **9a** (2-pentyl-2-hydroxy-1,2-dihydropyrrol-3-one) obtained most conveniently (56% isolated yield) using a slightly modified reaction condition, with separation from **1a** by extraction (see the Experimental Section). If **8** was incubated with butylamine using methanol rather than acetonitrile as cosolvent (1:1, v/v, with pH 4.75 sodium phosphate buffer), 2-pentyl-2-methoxy-1,2-dihydropyrrol-3-one (**10**) was isolated as the major product (45%) along with **1b**. Compounds **9a** and **10** are of substantial interest because, as discussed below, they are fluorescent with excitation/emission characteristics very similar to those of **1a**, and **9a** might be suspected as an intermediate in the generation of **1a**.

An alternative approach to **1a**, outlined in Scheme 4, started with the dimethylacetal **11** of HNE, synthesized according to known procedures.[34,35] Pyridinium chlorochromate (PCC) oxidation of **11** and subsequent deprotection afforded the desired (*E*)-4-oxo-2-nonenal (**13**) in 96% yield, which upon incubation with propylamine in pH 7.5 sodium phosphate buffer generated **1a** in 30% isolated yield. The ^{15}N-labeled **1a** discussed above was prepared from **13** and ^{15}N-labeled propylamine using this procedure.

In the reaction of **13** with propylamine, another major product (nonfluorescent) was formed in addition to **1a**. To simplify its structural characterization, an analogous reaction of (*E*)-4-oxo-2-pentenal (**14**) with ethylamine was employed. In the ^{1}H NMR spectrum of the resulting

(32) Butler, A. R.; Lioyd, D. *J. Chem. Soc. (B),* **1971**, 795−797.
(33) Favino, T. F.; Fronza, G.; Fuganti, C.; Fuganti, D.; Grasselli, P.; Mele, A. *J. Org. Chem.* **1996**, *61*, 8975−8979.
(34) Gree, R.; Tourbah, H.; Carrie, R. *Tetrahedron Lett.* **1986**, *27*, 4983−4986.
(35) Cox, C. M.; Whiting, D. A. *J. Chem. Soc., Perkin Trans. 1* **1991**, 1907−1911.

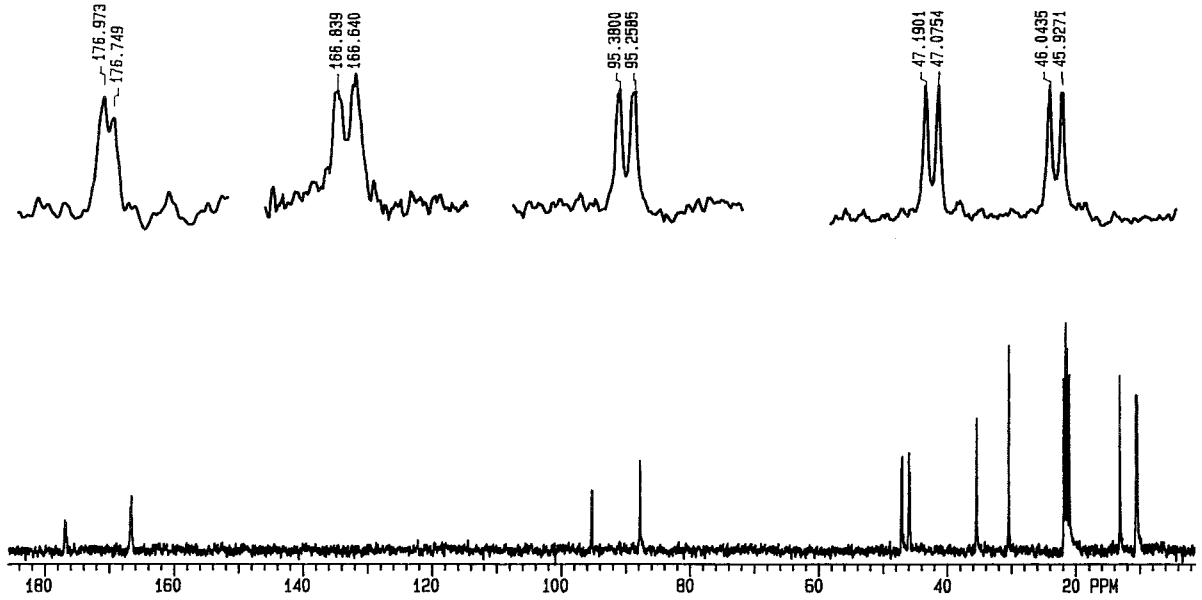

Figure 2. ^{13}C NMR spectrum of ^{15}N-labeled **1a** in $CDCl_3$.

Scheme 2

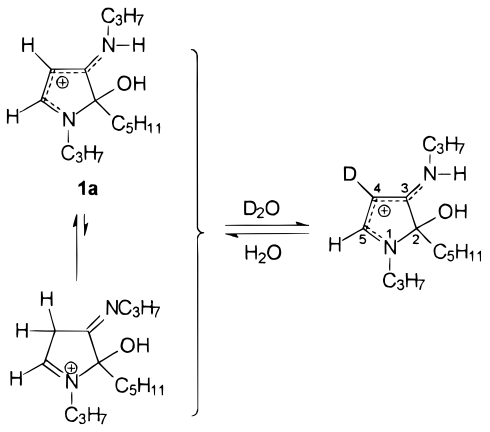

product **15a**, the appearance of two triplets at 1.50 and 1.30 ppm and two singlets at 1.68 and 1.87 ppm clearly indicated that two molecules each of amine and **14** were incorporated into the structure. HRMS confirmed that **15a** was a 2:2 adduct (M^+ at *m*/*z* 232.1572 corresponds to $C_{14}H_{20}N_2O$), and its ^{13}C NMR spectrum exhibited the expected 14 carbons. The $^1H-^1H$ COSY spectrum (Figure 3) indicated that the two doublets at 6.08 and 6.91 ppm are coupled (J = 5.70 Hz) and that the two doublets at 6.11 and 6.56 ppm are coupled (J = 2.90 Hz). The ^1H NMR pattern implicates a disubstituted pyrrole, where one substituent is a methyl group, and the other contains a −CH=CH− grouping. Considering the ppm separation of these coupled doublets and the corresponding ^{13}C NMR signals, we assign the former ^1H NMR doublets as the vinyl protons of an acrylamide rather than enaminone fragment, and the latter ^1H NMR doublets as pyrrole $\alpha\beta$ rather than $\alpha\beta'$ protons on the basis of the relatively large coupling constant. On the basis of this spectral data and a connectivity consistent with the precursor reactants, we assign the structure of the 2:2 dimer as **15a** shown in Scheme 5. Similarly, **15b** was isolated from reaction of **14** with propylamine. One plausible pathway to **15** involves condensation of **14** with one amine to give a 5-methyl-3-pyrrolin-2-one, which in its enol form undergoes conjugate addition to a second molecule of **14** at C-3,

Scheme 3[a]

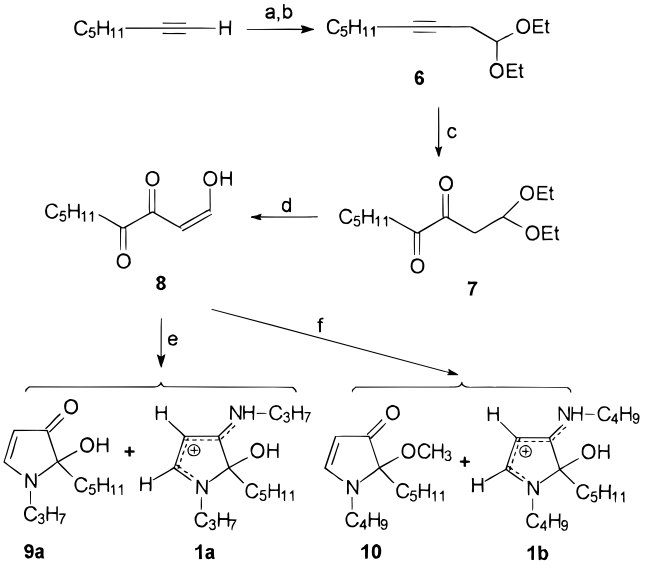

[a] Key: (a) BuLi, THF/HMPA (1:1, v/v), −78 °C; (b) $BrCH_2CH(OEt)_2$; (c) O_3/Me_2S, $CHCl_3$, −78 °C; (d) H_2O, HCl; (e) *n*-$PrNH_2$ in NaH_2PO_4 buffer (pH 4.75)/CN (3:1, v/v); (f) *n*-$BuNH_2$ in NaH_2PO_4 buffer (pH 4.75)/MeOH (1:1, v/v).

Scheme 4[a]

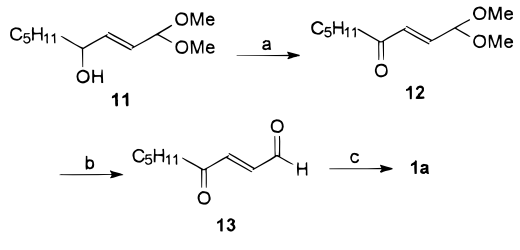

[a] Key: (a) PCC/NaOAc, CH_2Cl2; (b) H_2O, HCl; (c) *n*-$PrNH_2$ in NaH_2PO_4 buffer (pH 7.50), 0.4 mM $CuSO_4$.

followed by Paal−Knorr condensation of the resulting 4-keto aldehyde with the second amine.

4. Effects of pH, Solvent, and NMR Shift Reagent on the HNE- or HHE-Derived Fluorophores and

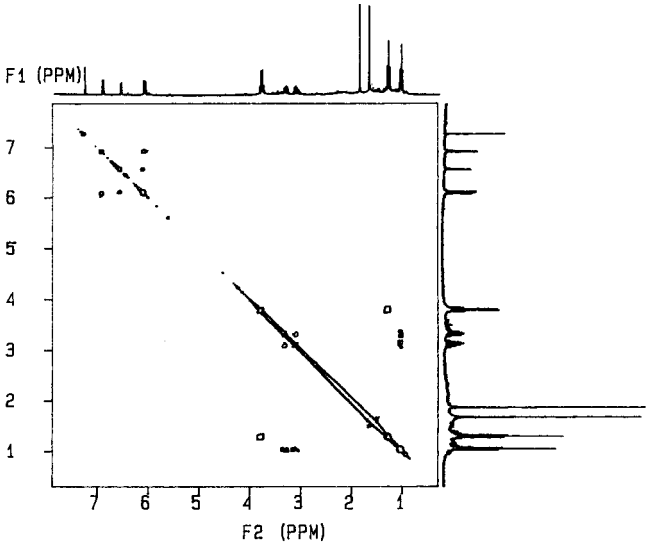

Figure 3. $^1H-^1H$ COSY NMR spectrum of **15a** in $CDCl_3$.

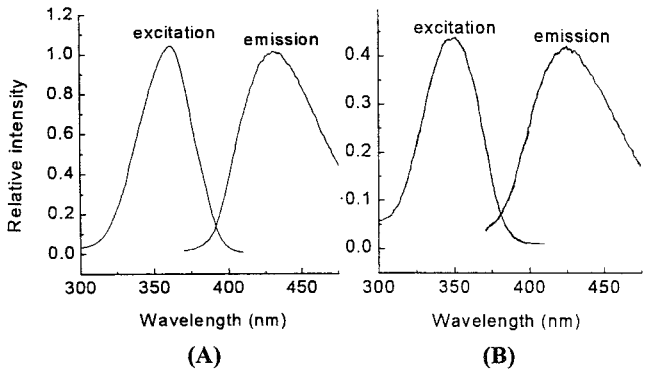

Figure 4. Fluorescence spectra for the isolated fluorophores **1a** (A) and **9a** (B).

Scheme 5

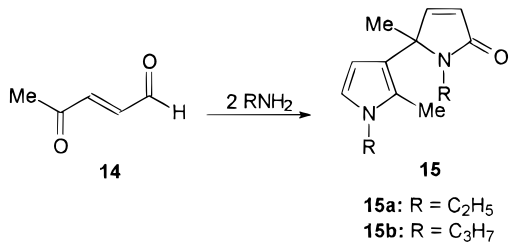

Their Analogues. The vinylogous amidinium **1** generated in the 4-hydroxy-2-alkenal-amine reaction systems exhibited fluorescence with ex/em maxima at 360/430 nm (Figure 4A). Compounds **1** are fairly stable in acidic, neutral, and slightly basic conditions, but there is a gradual decrease in fluorescence intensity between pH 9.0 and 9.5 and an abrupt decrease between pH 9.5 and 10.0 (Figure 5). This pH dependence resembled that of fluorescent pigments seen in aging as well as in the ceroid of atherosclerotic plaques.[1,38−40] The fluorescence intensity of **1** was totally quenched at pH ≥ 12. Rapid neutralization/acidification of base-exposed samples of **1** restored the ex/em 360/430 nm signature, though the extent to which this could be observed decreased both with increasing pH and the duration of base exposure prior to neutralization. We do not know whether the short-term reversible loss of chromophore represents merely deprotonation or reversible hydration prior to irreversible hydrolytic destruction.

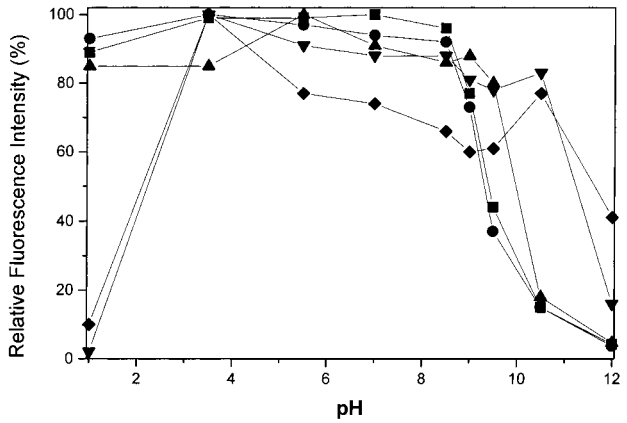

Figure 5. Effect of pH on the fluorescence intensity of 4-hydroxy-2-alkenal-derived fluorophores **1a** (■), **1b** (●), and **1c** (▲) and their analogues **9a** (▼) and **10** (♦).

Scheme 6

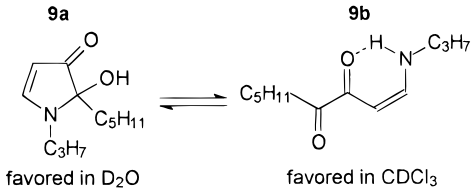

Interestingly, the 1:1 adducts **9a** and **10** that are generated alongside **1** in the reaction of amines with 3,4-dioxononanal (Scheme 3) have the same core structure as other adducts formed between amines and proposed lipoxidation products[36,37] and generate fluorescence at a wavelength (ex/em 350/428 nm) (Figure 4B) similar to that of **1**. However, the fluorescence of these 1:1 adducts was stable at pH 10 but quenched in an acidic medium (pH ≤ 3.5) (Figure 5), a trend opposite to that seen for **1** and age-related lipofuscin.[1,38−40] It is noteworthy that the fluorescence of **9a** is also solvent-dependent. In contrast to the exclusive presence of the fluorescent form **9a** in protic solvents such as methanol or water, the molecule exists in a nonfluorescent form in aprotic solvents, shown by ^1H NMR in $CDCl_3$ to be ring-opened tautomer **9b** (Scheme 6). This finding probably reflects the advantage of intramolecular hydrogen bonding in aprotic solvents, and its relative unimportance in protic solvents. Support for the tautomerization depicted in Scheme 6 is that **10**, being locked in its ring-closed form, does not lose its fluorescence upon change in solvent. The key observation is that the fluorescence properties of cyclic enaminones such as **9a** are not consistent with those observed in lipofuscin. Thus, despite the appropriate ex/em signature, such structures may not contribute significantly to age-related fluorescent pigments.

Another feature that has been used to characterize the naturally occurring fluorescence resulting from attachment of lipoxidation products to proteins and aminophos-

(36) Chen, P.; Wlesler, D.; Chmelik, J.; Novotny, M. *Chem. Res. Toxicol.* **1996**, *9*, 970−979.
(37) Fukuzawa, K.; Kishikawa, K.; Tokumura, A.; Tsukatani, H.; Shibuya, M. *Lipids* **1985**, 20, 854−861.
(38) Trombly, R.; Tappel, A. L. *Lipids* **1975**, *10*, 441−447.
(39) Trombly, R.; Tappel, A. L.; Coniglio, J. G.; Grogan, W. M., Jr.; Rhamy, R. K. *Lipids* **1975**, *10*, 591−596.
(40) Malshet, V. G.; Tappel, A. L.; Burns, V. M. *Lipids* **1974**, *9*, 328−332.

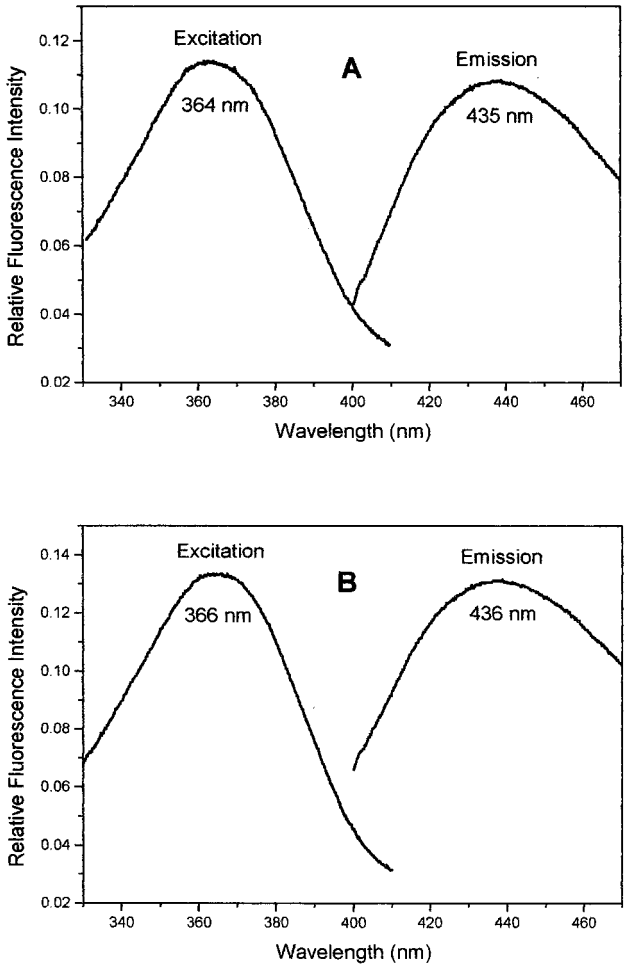

Figure 6. Fluorescence spectra of RNase A (1 mM) treated for 50 h with 1.5 mM HNE before (A) or after (B) protein denaturation (5% SDS).

pholipids is its reduction by coordination to lanthanide NMR shift reagents.[40] Consistent with the contribution of **1** to age-related fluorescence in vivo, we found that the fluorescence of **1b** in MeOH could be "titrated" with europium tris(6,6,7,7,8,8,8-heptafluoro-2,2-dimethyl-3,5-octanedionate) [Eu(fod)$_3$] (see the Experimental Section). Using a concentration of 37 μM **1b**, 0.1 mM Eu(fod)$_3$ gave an 18% reduction in fluorescence intensity, consistent with what has been observed for lipofuscin age pigments.[38−40]

5. Fluorophore Formation and Protein Cross-Linking from Incubation of Ribonuclease A (RNase A) with HNE. The ex/em 360/430 nm fluorophore is observed not only in the model reactions of HNE with primary amines but also in the reaction of HNE with proteins. Incubation of the 13.7 kDa protein RNase A (1 mM) with HNE (1.5 mM) for extended periods of time led to the appearance of a slightly red-shifted spectrum (Figure 6A) that, upon denaturing the protein, sharpened a little (Figure 6B). From the measured ΔA, using the ϵ_{360} measured for the model compounds **1** (1.3×10^4 M^{-1} cm^{-1}), it is possible to estimate that the yield of fluorophore accounts for 1.8% of total available lysines on the protein. The HNE-treated RNase also exhibited *covalent cross-linking* as assessed by sodium dodecyl sulfate−polyacrylamide gel electrophoresis (SDS−PAGE) (Figure 7). Molecular weight bands corresponding to RNase dimer, trimer, and even higher oligomers were observed

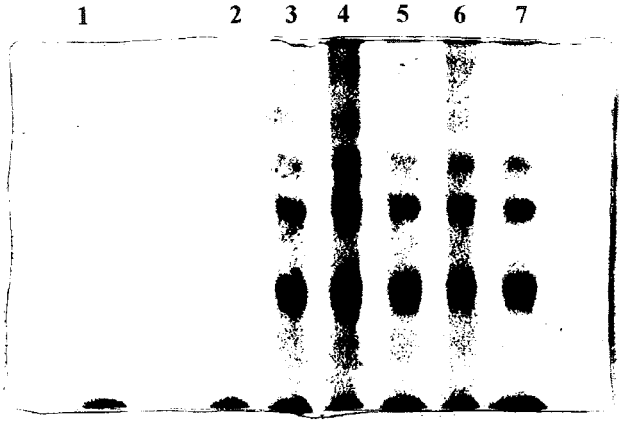

Figure 7. HNE-induced RNase A cross-linking. RNase A (lane 1) was incubated with either $CuSO_4$ (lane 2), HNE (lane 3), HNE in the presence of $CuSO_4$ (lane 4), HNE in the presence of both $CuSO_4$ and DTPA (lane 5), HNE in the presence of both $CuSO_4$ and DEF (lane 6), or HNE in the presence of DTPA alone (lane 7) under standard conditions described in the Experimental Section. Samples were denatured and analyzed by SDS−PAGE.

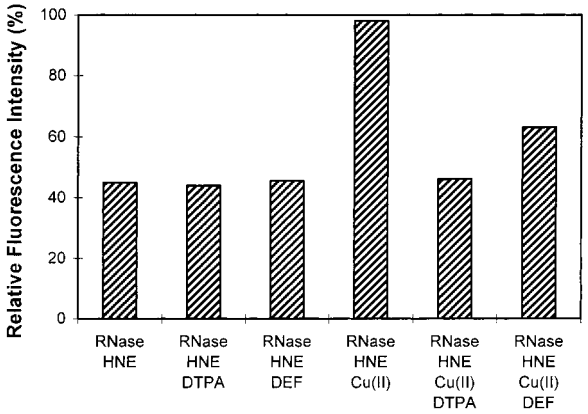

Figure 8. Relative fluorescence intensity exhibited by RNase A incubated with HNE alone or in the presence of the chelators DTPA or DEF and/or $CuSO_4$ (see the Experimental Section).

(Figure 7, lane 3). We showed independently that the A_{365} and emission intensity at 435 nm were unaffected upon heating the samples in electrophoresis denaturing buffer.

The presence of catalytic quantities of Cu(II) was found to substantially increase both RNase cross-linking (Figure 7, lane 4) as well as the RNase-associated fluorescence induced by HNE treatment (Figure 8). In addition, the strong Cu(II) chelator diethylenetriaminepentaacetic acid (DTPA) was found to abrogate the Cu(II)-induced increases in both cross-linking (Figure 7, lane 5) and fluorescence (Figure 8). The finding that DTPA inhibited only the Cu(II)-enhanced portion of cross-linking and fluorescence development and did not interfere with the remaining "background" portion suggests that there is both a Cu(II)-dependent and Cu(II)-independent mechanism leading to cross-linking and fluorescence. Consistent with this view, in the absence of added Cu(II), DTPA had little effect on the "background" level of HNE-mediated cross-linking (Figure 7, lane 7) or fluorescence development (Figure 8), ruling out adventitious trace copper as the factor underlying these observations. The iron-selective chelator deferoxamine (DEF) also failed to reduce the "background" level of HNE-mediated fluores-

cence (Figure 8) but only partially inhibited the Cu(II)-induced increases in both cross-linking (Figure 7, lane 6) and fluorescence (Figure 8). These experiments suggest that there may be a transition-metal-ion-independent autoxidation mechanism contributing to protein cross-linking and fluorophore generation occurring in the absence of added metal ions, even though atmospheric oxygen is an obligatory requirement for all cross-linking.

Copper(II) is the most frequently used catalyst for the in vitro preparation of oxidatively damaged LDL (ox-LDL).[30] This stems from the knowledge that Cu(II) is able to catalyze lipid oxidation, in part by stimulating the generation of reactive lipoxidation breakdown products (including 4-hydroxy-2-alkenals such as HNE) capable of modifying biomacromolecules.[9] Our observation here that Cu(II) promotes HNE-derived covalent cross-linking of RNase A suggests that the use of Cu(II) to catalyze direct protein oxidation[41] and lipid oxidation[30] should take into account that Cu(II) can also affect the late-stage covalent modification process. Because the resulting covalent protein cross-linking usually leads to protein aggregation and dysfunction as is seen in oxLDL, our findings suggest that the toxicity of HNE in vitro or in vivo may reflect the combined effects of HNE and adventitious trace transition metal ions.

Perhaps the most important implication of the above finding of a parallel response of fluorescence and cross-linking to the various experimental variables imposed on the HNE RNase reaction is that the fluorophore **1** (R = peptidyl lysine) could represent the major mechanism of protein cross-linking induced by HNE. Further studies will be needed to determine whether there are additional contributors to HNE-mediated cross-linking.

6. Hydride Reactivity of the HNE-Derived Fluorophore. We were interested in evaluating the stability of the fluorophore toward hydride reduction conditions that might be used in the reductive post-derivatization of HNE/HHE-treated proteins. Although the fluorescence of model compound **1a** remained unchanged in 50 mM $NaCNBH_3$ (phosphate buffer, pH 7.0), the fluorescence was quickly quenched by 10 mM $NaBH_4$ (in 1mM NaOH at 25 °C). Because the fluorophore is unstable to base alone, we carried out a study to assess the effect of $NaBH_4$ at more modest borate-buffered pH values (9−10), using RNase that was pretreated with HNE for 65 h to achieve the maximal level of fluorophore. As shown in Figure 9, both the absorbance at 360 nm and relative fluorescence intensity at 430 nm remained stable for 6 h when the HNE−RNase sample was diluted into pH 7.2 buffer but deteriorated about 40−50% over this same time period at pH 9 and completely at pH 10. In contrast, for the samples that were diluted into the same buffers followed by addition of 4 mg/mL $NaBH_4$, the absorbance and fluorescence declined much more rapidly. The distinguishing effect of borohydride reduction relative to base decomposition was clearly more evident at the lower pH value. We have not characterized the nature of the reduction product(s).

7. Studies on the Mechanism of Formation of the HNE-Derived Fluorophore. The reversibly formed Schiff base Michael adduct is not an intermediate. Previous studies revealed that the initial reaction of primary amines with HNE involves Michael addition at

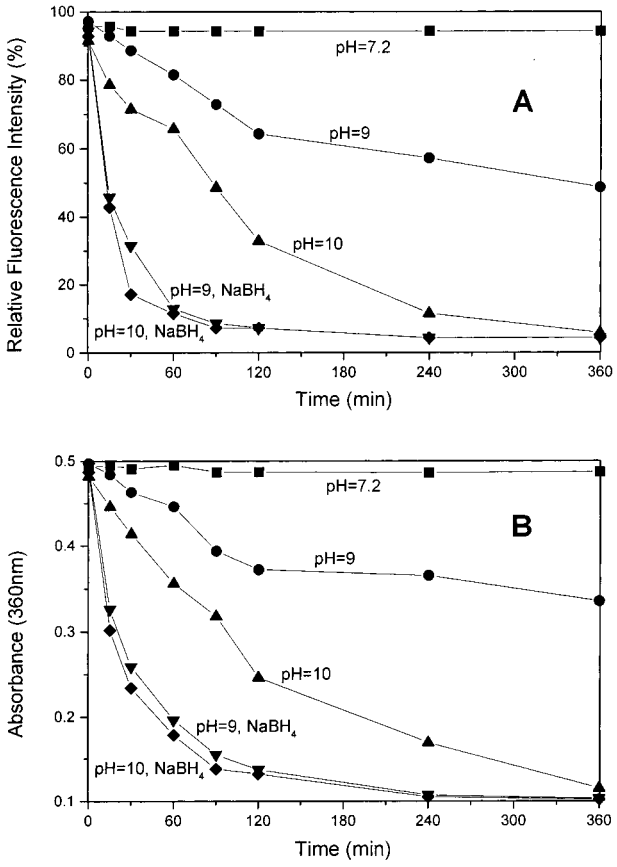

Figure 9. Relative fluorescence intensity (A) and absorbance at 360 nm (B) of RNase A that was treated with HNE for 65 h and then diluted into either pH 7.2 phosphate buffer (■), pH 9.0 borate buffer alone (●) or containing $NaBH_4$ (▼), or pH 10.0 borate buffer alone (▲) or containing $NaBH_4$ (♦). See the Experimental Section for details.

Scheme 7

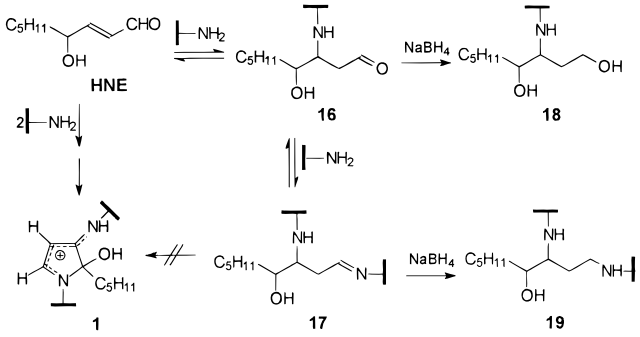

C-3 (1:1 amine/HNE adduct **16**) and Schiff base Michael adduct formation at C-1 and C-3 (2:1 amine/HNE adduct **17**)[42] (Scheme 7). These adducts are formed reversibly and can revert to amine and HNE in neutral aqueous buffer in the absence of reductive ($NaBH_4$) stabilization.[42] In contrast to this *reversible*, non-oxidative chemistry, generation of the HNE-derived fluorophore **1** represents an *irreversible* four-electron oxidation and depends on dioxygen as the ultimate electron acceptor. However, the C-1/C-3 amine connectivity present in **17** is preserved in the fluorophore **1**, so that one might propose the intermediacy of **17**, which subsequently undergoes a four-

(41) Berlett, R. S.; Stadtman, E. R. *J. Biol. Chem*. **1997**, *272*, 20313−20316.

(42) Nadkarni, D. V.; Sayre, L. M. *Chem. Res. Toxicol*. **1995**, *8*, 284−291.

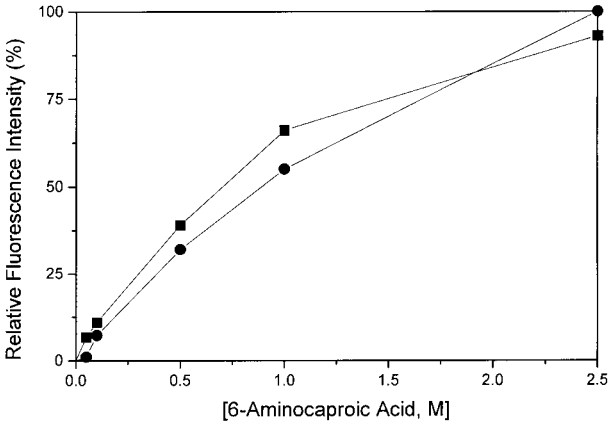

Figure 10. Effect of primary amine concentration on the relative yield of the fluorophore generated from treating 6-aminocaproic acid with either HNE (■) or HPE (●).

electron oxidative evolution to give **1**. In fact, both Itakura et al., who independently proposed generation of the same fluorophore (though as the free base),[28] and Tsai et al.[29] suggested without evidence that the Schiff base Michael adduct was the initial intermediate leading ultimately to the fluorophore.

Even when using excess amine, borohydride quenching of the reaction of amines with HNE results mainly in the reduced 1:1 amine Michael adduct **18**,[42] indicating that the 1:2 Schiff base Michael adduct **17** represents a minor equilibrium form in aqueous solution (Scheme 7). Thus, if the 1:2 adduct **17** were a direct precursor to the fluorophore, further increasing the amine concentration should linearly increase the proportion of 1:2 adduct **17** and thereby result in an increase in yield of fluorophore with time. We found that the fluorescence intensity after 144 h in the reactions of both HNE and HPE with 6-aminocaproic acid as a lysine mimic reflected this expectation (Figure 10), consistent with the possibility that the 1:2 adduct **17** is an intermediate on the pathway to the fluorophore. However, because the fluorophore represents a 1:2 adduct, one might expect an increase in its time-dependent yield upon increasing amine concentration, whether **17** was on the pathway to **1** or merely represented a side-equilibrium. Thus we needed a different approach to confirm whether **17** was an obligatory precursor to **1**. Ultimately, we excluded **17** as a direct intermediate to **1** on the basis of the following set of experiments.

In the model reaction of HNE (40 mM) with butylamine (320 mM), we observed that the ex/em 360/430 nm fluorescence increased during the initial 48 h then slowed and reached a maximum after 96 h (Figure 11). In addition, the yield of fluorophore monitored by HPLC paralleled the fluorescence intensity (Figure 11), confirming that **1b** is the major contributor to the fluorescence over this time span. At 144 h into the reaction, after the fluorescence had clearly plateaued, we quenched the HNE−butylamine reaction mixture with $NaBH_4$ and then analyzed the reduced products. The same quench analysis was performed at an early time (24 h), when the fluorescence was still increasing. As shown in Table 1, we isolated the reduced 1:1 adduct **18** as the major reduced product and reduced 1:2 adduct **19** as the minor one, and *this ratio did not change between the 24 and 144 h quench points.* If **17** had been an intermediate to **1b** as suggested,[28,29] it should have been consumed by

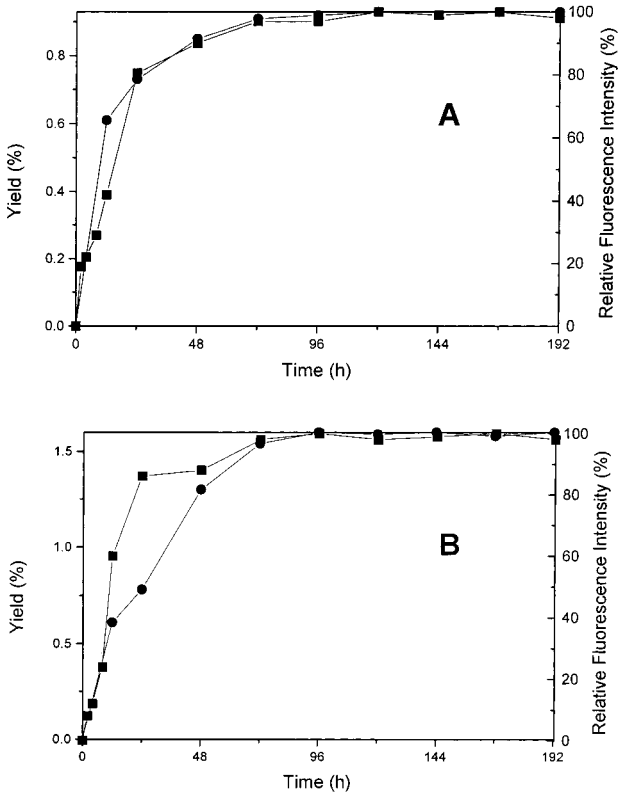

Figure 11. Time course of generation of the fluorophore in the reaction of butylamine with HNE (A) (giving **1b**) or the reaction of ethylamine with HPE (B), as assessed by either relative fluorescence intensity (■) or HPLC quantitation (●).

Table 1. Yields of the Borohydride-Reduced 1:1 and 2:1 Amine/4-Hydroxy-2-alkenal Adducts[a]

	24 h	144 h
1:1 butylamine-HNE	61%	69%
:2 butylamine-HNE	4.7%	6.0%
1:1 ethylamine-HPE	63%	72%
1:2 ethylamine-HPE	4.2%	4.5%

[a] The % yield figures were obtained by (i) determining the ratio of the reduced 1:1 and 1:2 adducts from the crude ^{1}H NMR spectrum following workup and (ii) determining the overall yield of the two products by preparative TLC isolation, as described in the Experimental Section.

the time that the ex/em 360/430 nm fluorescence and HPLC-determined **1b** yield had reached their maxima. In these experiments, we presume that the ratio of reduced products obtained reflects the equilibrium ratio of 1:1 and 1:2 adducts prior to the borohydride quench. Thus, our isolation of the reduced 2:1 Schiff base Michael adduct **19** demonstrated that its precursor **17** was still present in the reaction solution and should be continuing to evolve to **1b** if it were an intermediate on the pathway to **1b**. In fact, our experimental result implies that both the 1:1 and 2:1 adducts **16** and **17** represent HNE being tied up in forms that do not revert to HNE under these excess amine reaction conditions, despite their clear reversibility upon attempted isolation.[42] We are forced to conclude that the formation of fluorophore **1** in aqueous solution from HNE and amines represents a reaction pathway that ceases as soon as free HNE in solution is depleted.

Because of the hydrophobicity of HNE, one might argue that its Schiff base Michael adduct **17** is also hydrophobic and may become effectively separated from the aqueous

Scheme 8

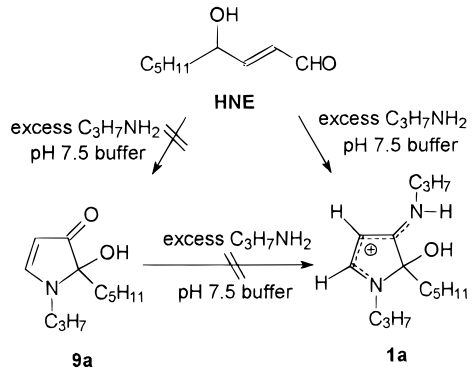

reaction solution at some point in time, such that the formation of the ex/em 360/430 nm fluorophore ceases for this reason. Though we saw no evidence of phase separation, we could not exclude the presence of micelles. To control for a phase separation possibility, we thus repeated the same reaction and reductive quench experiment with HPE instead of HNE and ethylamine instead of butylamine. Using these more hydrophilic reactants, we observed nearly the same distribution of reduced 1:1 and 1:2 adducts (**20/21**) as in the previous case (Table 1). These results provide compelling evidence against the Schiff base Michael adduct being an intermediate on the reaction pathway leading to fluorophore **1**.

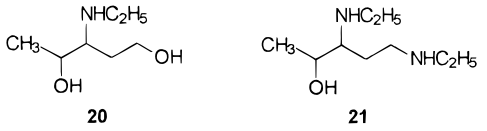

8. The 2-Pentyl-2-hydroxy-1,2-dihydropyrrol-3-one (9a) is Neither a Product of the HNE−Amine Reaction nor an Intermediate to Fluorophore 1. In our independent synthesis of **1** starting from 3,4-dioxononanal, we also isolated the 1:1 adduct **9a**, which exhibited similar fluorescence (ex/em 350/428 nm) (Scheme 4). Because its core structure has been claimed to be formed from lipoxidation-derived alkanals,[36,37] it is necessary to investigate whether **9a** is a product of the HNE−propylamine reaction and/or a precursor to the iminium derivative **1a**. Incubation of HNE with excess propylamine in sodium phosphate buffer (pH 7.5) yielded no detectable **9a** by HPLC (Scheme 8). In addition, independently prepared **9a** did not lead to the formation of any **1a** under reaction conditions identical to those where **1a** forms starting with HNE. It appears that the resonance stablized enaminone structure of **9a** is unreactive toward amines once it forms. Thus, **9a** is neither a product of the HNE−propylamine reaction nor an intermediate for **1a** formation.

9. Proposed Mechanism of 4-Hydroxy-2-alkenal-Derived Fluorophore Formation. We previously reported that Schiff base condensation at C-1 of HNE, though a minor kinetic pathway, leads irreversibly in part to a 2-pentylpyrrole.[31] In Scheme 9, we propose a branching of the enamine tautomerization of the initial Schiff base, leading either to pyrrole (via dehydration) or to fluorophore (via two 2e oxidations). We believe that the ability to form vinylogus enol/enamine intermediates **22a** and **22b** is requisite to the oxidation process, in analogy with the two-electron enediol oxidation seen for vitamin C[43] and monosaccharide autoxidation.[44] The low yield of fluorophore **1** could reflect in part an unfavorable equilibrium constant *K* for conversion of the initial Schiff base to the enamine, a step that may be sensitive to buffer and pH.

The pathway we speculate in Scheme 9 is consistent with our efforts to obtain the HNE-derived fluorophore by independently accessing more advanced intermediates in the proposed mechanism, using alternate starting compounds **13** and **8**. The promotion of fluorophore **1** development by Cu(II) may arise from its catalysis of these oxidations. During our further investigation of the reaction of HNE or HHE with 2-methoxyethylamine, we found that the presence of Cu(II) has an *inhibitory* effect on the formation of the corresponding pyrrole end products **23a** or **23b**, respectively, even though it can promote formation of the corresponding ex/em 360/430 nm fluorophores **1d** or **1e** (Table 2). This finding is consistent with both pyrrole and fluorophore being generated from the same proposed intermediate in Scheme 9 (**22a** for HNE). In this case, the role of Cu(II) is to accelerate the oxidation step, converting more intermediate **22a** into fluorescent adduct **1d**, thereby indirectly inhibiting formation of pyrrole **23a**.

Although both 3,4-dioxo-nonanal (**8**) and (*E*)-4-oxo-2-nonenal (**13**) can lead to the proposed "advanced intermediates" suggested in Scheme 9 and can produce the same HNE-derived fluorophore **1**, they must not be directly involved in their free forms as intermediates starting from HNE. This is because we observed that **8** and **13** also generate **9a** and **14a**,**b**, respectively, which are not found in the corresponding HNE−amine reactions (data not shown).

Our data bearing on the possibility of both metal-dependent and -independent autoxidative pathways is not readily interpretable in terms of Scheme 9 at the level of detail shown, and more work will be required to understand this point as well as the question of reversibility of the 1:1 Michael adduct and 2:1 Schiff base Michael adduct in the reaction solution in which fluorophore **1** is generated.

Conclusion

The findings reported here imply that the condensation between lipoxidation-derived reactive aldehydes and protein lysine groups might represent a process common to the formation of lipofuscin in aging and ceroid in atherosclerotic plaques. The importance of the 4-hydroxy-2-alkenal-derived ex/em 360/430 nm fluorophore as a marker of lipoxidative stress and as a potential contributor to fluorescent age-associated pigmentation and to pathologic cross-linking of proteins in vivo warrants additional work to confirm its physiologic occurrence and significance.

Experimental Section

General. Ribonuclease A from bovine pancreas Type III-A was obtained from Sigma (St. Louis, MO) and used as received.

(43) (a) Taqui Khan, M. M.; Martell, A. E. *J. Am. Chem. Soc.* **1967**, *89*, 4176−4185. (b) Taqui Khan, M. M.; Martell, A. E. *J. Am. Chem. Soc.* **1967**, *89*, 7104−7111.

(44) Thornalley, P.; Wolff, S.; Crabbe, J.; Stern, A. *Biochim. Biophys. Acta* **1984**, *797*, 276−287.

Scheme 9

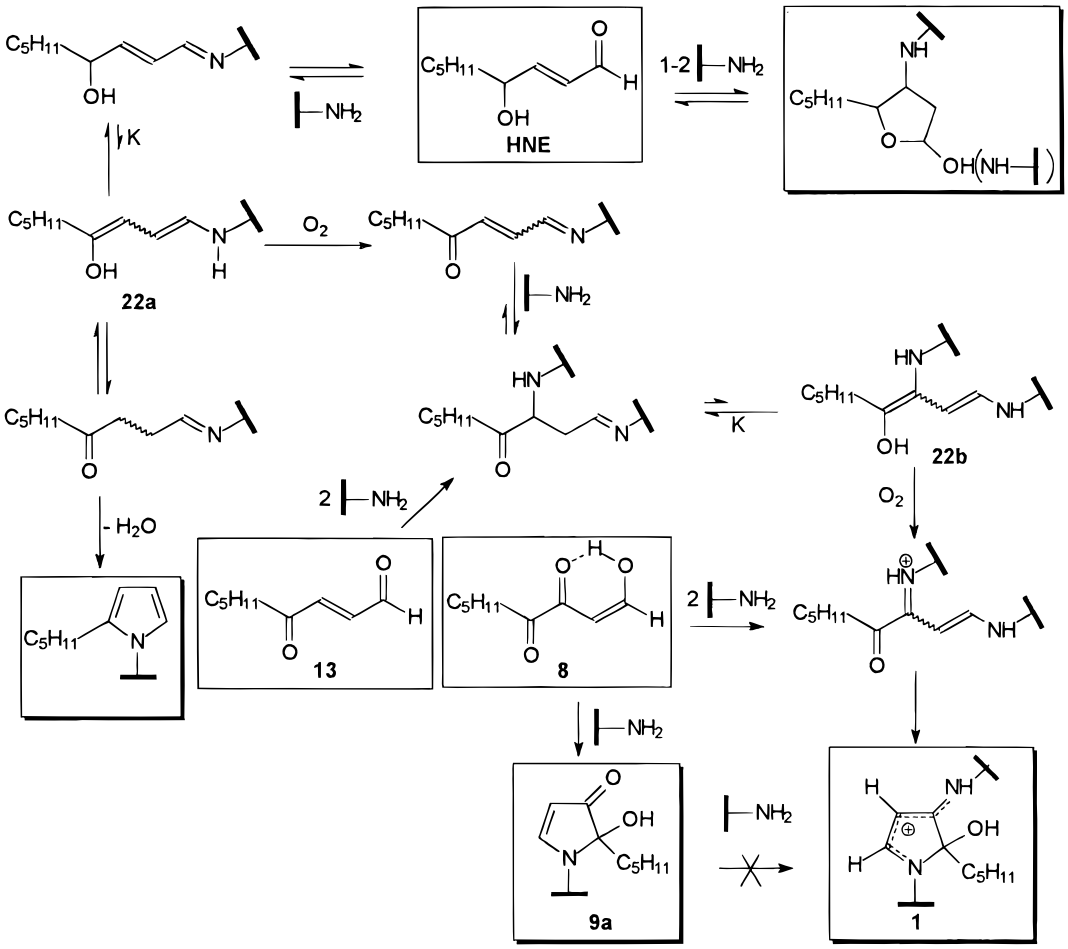

Table 2. Effects of Cu(II) on HPLC Yields (%) of Pyrroles and Fluorophores

	HNE−2-methoxyethylamine				HHE−2-methoxyethylamine			
	pyrrole **23a**		fluorophore **1d**		pyrrole **23b**		fluorophore **1e**	
	+ Cu(II)	− Cu(II)	+ Cu(II)	− Cu(II)	+ Cu(II)	− Cu(II)	+ Cu(II)	− Cu(II)
pH 7.5	0.17	1.50	1.20	0.27	0.37	2.00	1.80	0.31
pH 8.5	0.13	1.07	0.73	0.18	0.24	1.20	1.10	0.20
pH 9.5	0.09	0.20	0.22	0.04	0.17	0.18	0.13	0.05

Electrophoresis studies utilized an SE 200 Series minigel castor (Hoefer Scientific Instruments, San Francisco, CA) and a Fisher Biotech FB 570 power supply (Fisher Scientific, Pittsburgh, PA). All buffer solutions were made with distilled water purified by a type D4700 NANOpure Bioresearch Deionization System (Barnstead/Thermolyne Corporation, Dubuque, IA). All reactions were carried out with continuous magnetic stirring under an atmosphere of dry nitrogen at room temperature unless otherwise noted, and all evaporations were carried out at reduced pressure with a rotary evaporator at ca. 30 Torr. HNE, HHE, and HPE were prepared according to a recent literature procedure.[34,35] All other materials were reagent grade.

Spectroscopy. ^{1}H NMR (300 MHz), ^{13}C NMR (75.1 MHz), and ^{1}H−^{1}H correlation spectroscopy (COSY) were recorded on a Varian Gemini 300 instrument. In all cases, tetramethylsilane or the solvent peak served as an internal standard for reporting chemical shifts, expressed on the δ scale. In the ^{13}C NMR line listings, attached proton test (APT) designations are given as (+) or (−) following the chemical shift. When appropriate, the samples for proton NMR spectroscopy were deuterium-exchanged three times with CD_3OD under a nitrogen atmosphere. High-resolution mass spectra (HRMS) were obtained at 20 eV on a Kratos MS-25A instrument. UV spectra were obtained with a Perkin-Elmer model Lambda 3B spectrophotometer fitted with a water-jacketed multiple cell holder for maintenance of constant temperature. Fluorescence spectra were recorded on a SLM8100C spectrofluorometer. A slit width of 5 nm was used, and the fluorescence intensity was standardized with quinine sulfate (0.1 μM in 0.1 N H_2SO_4). Relative fluorescence intensity measurements were determined using an Aminco-Bowman spectrofluorometer.

High-Performance Liquid Chromatography (HPLC). Samples were filtered through a 0.22 μm (pore size) GV-type filter (Millipore Corporation, Milford, MA) prior to injection. The HPLC system (Shimadzu Corporation, Kyoto, Japan) consisted of two LC-6A pumps, an automatic gradient controller (model SCL-6A), a model SIL-1A manual injector and a model C-R3A integrator. Analytical separations were carried out using a 4.0 mm × 30 mm C_{18} reverse-phase column (MCH 10 10 μm) (Varian Associates, Palo Alto, CA). The solvent system consisted of 50 mM Et_3N/HOAc (1:1) (A) and MeOH (B). The program was as follows: 0−30 min, 65−40% A; 30−40 min, 40−35% A, 40−60 min, 35% A. The flow rate was set at 1.0 mL/min, and the column effluent was monitored for absorbance at 355−365 nm or 230−280 nm with a multiple wavelength detector (HP 1050 series, Hewlett-Packard company, Waldbronn Analytical Division, Waldbronn, Germany). Semipreparative scale separation was achieved with 8 mm × 100 mm RCM 8 × 10 radical PAK cartridges (Waters Chro-

matography, Millipore Corporation, Milford, MA); packing: resolve C_{18}, 10 μm. The solvent system consisted of 0.1% trifluoroacetic acid (TFA) in water (A) and MeOH (B). The program was as follows: 0−30 min, 65−35% A; 30−40 min, 35%A; 40−45 min, 30−25% A. The flow rate was set at 2.0 mL/min, and the effluent was monitored for absorbance at 355−365 nm.

Quantitative Comparison of Fluorophore Formation Derived from HNE or HHE with *n*-Butylamine at Different Reaction Conditions. A solution of 15.6 mg (0.10 mmol) of HNE or 11.4 mg (0.10 mmol) of HHE in MeOH (0.5 mL) was added to 2 mL of a solution containing 0.02−0.50 mmol of *n*-$BuNH_2$ with or without 1% $CuSO_4$/2,2′-bipyridine (based on amine) at pH 7.5, 8.5, and 9.5, where the pH was established by adding NaH_2PO_4 to the amine solution. Each mixture was kept stirring at room temperature open to the atmosphere. At the indicated time points, 10 μL of solution was analyzed by analytical RP-HPLC and monitored by the absorbance at 355−365 nm. Quantitative analysis was based on the peak height. To investigate the effects of antioxidants on fluorophore formation, 4-*tert*-butylphenol or vitamin C (40 mM final concentration) was added to the HNE−*n*-butylamine (1:5 molar ratio) reaction mixture. In a separate experiment, 2.5 mL of reaction solution containing 0.1 mmol HNE and 0.5 mmol *n*-$BuNH_2$ was subjected to two freeze−pump−thaw cycles under argon, followed by capping: after 72 h of incubation, analysis by analytical RP-HPLC and absorbance at 355−365 nm indicated the complete absence of fluorophore **1b**.

Reaction of HNE or HHE with Primary Amines and Isolation of 1. A primary amine (*n*-butylamine and *n*-propylamine, 80 mmol) in 200 mL of water was neutralized to pH 7.5 by adding NaH_2PO_4. To this air-saturated amine solution were added 8.5 mg (0.05 mmol) of $CuCl_2 \cdot 2H_2O$ and 15.6 mg (0.10 mmol) of 2,2′-bipyridine. After the $CuCl_2$/2,2′-bipyridine complex was totally dissolved into the solution, a solution of either 1.56 g (10 mmol) of HNE or 1.14 g (10 mmol) of HHE in 50 mL of acetonitrile was added. The reaction mixture was stirred aerobically and monitored by spectrofluorometry and analytical reverse-phase HPLC. When generation of fluorophore plateaued (∼3 d), the mixture was concentrated under reduced pressure. The resulting syrupy residue was extracted with methanol. The combined methanol extracts were evaporated to a volume of 15 mL and then subjected to reverse-phase semipreparative HPLC separation. The fluorescent fractions were pooled and further purified by flash chromatography (MeOH/EtoAc 4:1, v/v, as eluent). The isolated fluorescent compounds all exhibited ex/em 360/430 nm fluorescence. Compounds **1b** and **1c** were isolated and characterized in our previous paper.[27] For **1a** (from HNE and propylamine) the yield was 4.6 mg (0.18% based on starting HNE). UV $\lambda_{max} = 360$ nm, $\epsilon_{360} = 1.3 \times 10^4\ M^{-1}\ cm^{-1}$ in pH 7.4 sodium phosphate buffer. ^{1}H NMR (D_2O) δ 0.87 (t, J = 6.78 Hz, 3H), 0.98 (t, J = 7.41 Hz, 3H), 0.99 (t, J = 7.38 Hz, 3H), 1.24−1.32 (m, 4H), 1.61−1.92 (m, 7H), 2.06−2.17 (m, 1H), 3.35 (t, J = 6.86 Hz, 2H), 3.45 (t, J = 7.43 Hz, 2H), 5.48 (d, J = 3.06 Hz, 1H, exchangeable), 8.28 (d, J = 3.03 Hz, 1H); ^{13}C NMR (D_2O) δ 10.47 (−), 10.62 (−), 13.20 (−), 21.00 (+), 21.87 (+), 22.35 (+), 22.56 (+), 31.32 (+), 36.19 (+), 46.19 (+), 47.70 (+), 87.76 (−), 95.86 (+), 166.57 (−), 176.70 (+); HRMS calcd for $C_{15}H_{29}N_2O$ 253.2280, found 253.2278.

***N,N′*-Dipropyl-2-methoxy-2-pentyl-1,2-dihydropyrrol-3-one Iminium (5).** Compound **1a** is partially converted into **5** upon standing in MeOH over silica gel for 48 h. Compound **5** was then isolated by flash chromatography with 1:1 MeOH/EtOAc as eluent. ^{1}H NMR (D_2O) δ 0.81 (t, J = 7.2 Hz, 3H), 0.94 (t, J = 7.35 Hz, 3H), 0.98 (t, J = 7.2 Hz, 3H), 1.19−1.25 (m, 4H), 1.62−1.88 (m, 7H), 2.03−2.14 (m, 1H), 3.09 (s, 3H), 3.35 (t, J = 7.5 Hz, 2H), 3.38 (t, J = 6.9 Hz, 2H), 5.60 (d, J = 3.3 Hz, 1H), 8.33 (d, J = 3.3 Hz, 1H); ^{13}C NMR (D_2O) δ 10.57 (−), 10.77 (−), 13.14 (−), 20.99 (+), 21.26 (+), 21.41 (+), 21.66 (+), 30.48 (+), 35.47 (+), 45.88 (+), 47.33 (+), 52.30 (−), 90.28 (−), 100.19 (+), 168.37 (−), 174.40 (+); HRMS cacld for $C_{16}H_{31}N_2O$ 267.2438, found 267.2431.

1,1-Diethoxy-3-nonyne (6). A solution of 2.5 M *n*-butyllithium in hexane (8 mL, 20 mmol) was added into a solution of 1-heptyne (1.92 g, 20 mmol) in 1:1 THF/HMPA (40 mL) under nitrogen at −78 °C. The temperature was raised to −45 °C for 45 min and relowered to −78 °C, and a solution of bromoacetaldehyde diethyl acetal (3.94 g, 20 mmol) in THF (10 mL) was added dropwise. After stirring and warming from −78 °C to room temperature over 20 h, the reaction mixture was concentrated, diluted with 30 mL of aqueous NH_4Cl, and extracted with ethyl ether (3 × 40 mL). The combined extracts were washed with brine and water, dried over anhydrous Na_2SO_4, and concentrated under reduced pressure to afford a brown residue which was purified by flash column chromatography on silica gel using 1:1 EtOAc/hexane to give **6** (4.07 g, 96%) as yellow oil. ^{1}H NMR ($CDCl_3$) δ 0.86 (t, J = 6.87 Hz, 3H), 1.19 (t, J = 7.05 Hz, 6H), 1.26−1.38 (m, 4H), 1.39−1.50 (m, 2H), 2.12 (t, J = 6.99 Hz, 2H), 2.46 (app d, J = 5.61 Hz, 2H), 3.53 (dq, J = 8.2 and 7.1 Hz, 2H), 3.65 (dq, J = 8.2 and 7.2 Hz, 2H), 4.58 (t, J = 5.76 Hz, 1H); ^{13}C NMR ($CDCl_3$) δ 13.89 (−), 15.17 (−), 18.70 (+), 22.18 (+), 25.02 (+), 28.60 (+), 30.99 (+), 61.62 (+), 75.14 (+), 81.80 (+), 101.32 (−); HRMS calcd for ($C_{13}H_{24}O_2 - C_2H_5O$) 167.1437, found 167.1436.

1,1-Diethoxy-3,4-Nonanedione (7). Ozonized oxygen was bubbled through a solution of of 1,1-diethoxy-3-nonyne (2.12 g, 10 mmol) in $CHCl_3$ (50 mL) at −78 °C. When the persistence of blue color signaled complete reaction, the reaction solution was flushed with nitrogen for 10 min, and then Me_2S (1.47 mL, 20 mmol) was added. After 4 h, the reaction mixture was partitioned between $CHCl_3$ and water, the orgainc layer was concentrated under reduced pressure, and the residue was purified by flash column chromatography with 1:2 EtOAc/hexane as eluent to afford **7** (2.24 g, 92%). ^{1}H NMR ($CDCl_3$) δ 0.86 (t, J = 6.75 Hz, 3H), 1.14 (t, J = 7.11 Hz, 6H), 1.24−1.32 (m, 4H), 1.50−1.59 (m, 2H), 2.68 (t, J = 7.31 Hz, 2H), 3.03 (d, J = 5.94 Hz, 2H), 3.48 (dq, J = 8.2 and 7.1 Hz, 2H), 3.61 (dq, J = 8.2 and 7.0 Hz, 2H), 4.93 (t, J = 5.79 Hz, 1H); ^{13}C NMR ($CDCl_3$) δ 13.80 (−), 15.10 (−), 22.22 (+), 22.60 (+), 31.26 (+), 35.83(+), 41.27 (+), 61.78 (+), 99.16 (−), 196.81 (+), 199.82 (+); HRMS calcd for $C_{13}H_{24}O_4$ 244.1675, $C_{11}H_{19}O_3$ ($M^+ - C_2H_5O$) 199.1335, found 199.1338.

3,4-Dioxononanal (8). To a solution of 2 N HCl (10 mL) in acetone (20 mL) was added **7** (1.0 g, 41 mmol). The reaction mixture was stirred at room temperature for 1 h, and then acetone was removed from it under reduced pressure. The aqueous residue was extracted with CH_2Cl_2 (4 × 10 mL). The combined extracts were evaporated under reduced pressure to afford **8** (0.68 g, 99%), which exists exclusively in its enol form in $CHCl_3$. ^{1}H NMR ($CDCl_3$) δ 0.83 (t, J = 6.8 Hz, 3H), 1.21−1.29 (m, 4H), 1.52−1.62 (m, 2H), 2.75 (t, J = 7.3 Hz, 2H), 6.18 (d, J = 3.6 Hz, 1H), 8.61, (d, J = 3.3 Hz, 1H); ^{13}C NMR δ 13.89 (−), 22.41 (+), 22.87 (+), 31.27 (+), 36.92 (+), 98.63 (−), 184.28 (−), 196.70 (+), 199.79 (+); HRMS calcd for $C_9H_{14}O_3$ 170.0943, found 170. 0939.

Reaction of 8 with *n*-Propylamine in Aqueous Acetonitrile. A solution of *n*-propylamine (590 mg, 10 mmol) in 30 mL of water was neutralized to pH 4.75 with NaH_2PO_4, and then freshly prepared **8** (170 mg, 1 mmol) in 10 mL of acetonitrile was added. Strong fluorescence developed within a few minutes. The reaction mixture was incubated for 16 h, concentrated, and extracted with EtOAc (3 × 20 mL). The water layer was concentrated and subjected to semipreparative HPLC purification. The effluent was monitored for absorbance at 355−365 nm. Compound **1a** was isolated in 27.6% yield (70 mg) and shown to be identical with that isolated from the incubation of HNE with propylamine in all respects (NMR, HRMS). The combined EtOAc extracts were concentrated, and the crude residue was purified by flash chromatography (EtOAc as eluent) to afford a fast-moving nonfluorescent fraction and a slow-moving fluorescent fraction. NMR of the slow-moving fluorescent fraction in CD_3OD indicated it to be ***N*-propyl-2-pentyl-2-hydroxy-1,2-dihydropyrrol-3-one (9a)**: ^{1}H NMR (CD_3OD) δ 0.90 (t, J = 6.9 Hz, 3H), 0.98 (t, J = 7.3 Hz, 3H), 1.21−1.39 (m, 6H), 1.65−1.85 (m, 4H), 3.30 (t, J = 7.4 Hz, 2H), 4.97 (d, J = 3.5 Hz, 1H), 8.22 (d, J = 3.5 Hz, 1H); ^{13}C NMR (CD_3OD) δ 11.74 (−), 14.37 (−), 23.35 (+), 23.60 (+), 23.91 (+), 32.94 (+), 35.89 (+), 47.51 (+), 91.93 (+), 94.74

(−), 168.86 (−), 204.42 (+); HRMS calcd for $C_{12}H_{21}NO_2$ 211.1573, found 211.1574. The NMR spectra of the nonfluorescent fraction in $CDCl_3$ indicated it to be the ring-opened form **1-(propylamino)-1-nonene-3,4-dione (9b)**: ^{1}H NMR ($CDCl_3$) δ 0.87 (t, J = 6.81 Hz, 3H), 0.95 (t, J = 7.40 Hz, 3H), 1.23−1.32 (m, 6H), 1.55−1.64 (m, 4H), 3.24 (q, J = 6.61 Hz, 2H), 5.68 (d, J = 7.08 Hz, 1H), 7.06 (dd, J = 13.11 and 7.08 Hz, 1H), 10.42 (br, 1H). Evaporation of the CD_3OD solution of **9a** and dissolution in $CDCl_3$ revealed its tautomerization to **9b**. The combined yield of the two tautomers was 250 mg (59%).

Reaction of 8 with *n*-Butylamine in Aqueous Methanol. A solution of *n*-butylamine (860 mg, 11.8 mmol) in water (10 mL) was neutralized to pH 4.75 with NaH_2PO_4. To this amine solution was added freshly prepared **8** (200 mg, 1.2 mmol) in 10 mL of MeOH, at which point the mixture turned brown. After 16 h, the mixture was concentrated and extracted with EtOAc. The water layer was evaporated under reduced pressure, and the residue was dissolved in a minimal amount of MeOH. This solution was subjected to semipreparative HPLC purification. The eluent was monitored for absorbance at 355−365 nm. Compound **1b** was isolated in 17% yield (51 mg) and shown to be identical with that isolated from the incubation of HNE with butylamine in all respects (NMR, HRMS). The EtOAc extracts were evaporated, and the crude residue was purified by flash chromatography (EtOAc as mobile phase) to afford fluorescent product ***N*-butyl-2-pentyl-2-methoxy-1,2-dihydropyrrol-3-one (10)** in 45% yield (120 mg). ^{1}H NMR(CD_3OD) δ 0.88 (t, J = 6.89 Hz, 3H), 1.02 (t, J = 7.29 Hz, 3H), 1.04−1.13 (m, 2H), 1.23−1.33 (m, 4H), 1.39−1.51 (m, 2H), 1.69−1.82 (m, 4H), 3.09 (s, 3H), 3.29 (t, J = 7.73 Hz, 2H), 5.07 (d, J = 3.66 Hz, 1H), 8.40 (d, J = 3.54 Hz, 1H); ^{13}C NMR(CD_3OD) δ 14.18(−), 14.36 (−), 21.34 (+), 23.12 (+), 23.56 (+), 32.28 (+), 32.92 (+), 35.59 (+), 45.54 (+), 52.36 (−), 96.77 (+), 97.32 (−), 170.37 (−), 202.52 (+); HRMS calcd for $C_{14}H_{25}NO_2$ 239.1887, found 239.1885.

(*E*)-1,1-Dimethoxy-2-nonen-4-one (12). A solution of HNE dimethyl acetal (**11**) (0.5 g, 2.45 mmol) in 20 mL of dry CH_2Cl_2 was added dropwise to a well-stirred solution of pyridinium chlorochromate (1.06 g, 4.90 mmol) in dry CH_2Cl_2 containing 1.5 g of NaOAc. After 6 h the mixture was concentrated, and the dark residue was diluted with 250 mL of dry ether and filtered through cotton gauze. Upon evaporation of solvent, the residue was purified by flash chromatography (EtOAc as eluent) to yield 460 mg (96%) of **12**.^{1}H NMR ($CDCl_3$) δ 0.85 (t, J = 6.8 Hz, 3H), 1.20−1.32 (m, 4H), 1.53−1.63 (m, 2H), 2.53 (t, J = 7.4 Hz, 2H), 3.31 (s, 6H), 4.99 (dd, J = 3.8 and 1.1 Hz, 1H), 6.33 (dd, J = 16.6 and 1.1 Hz, 1H), 6.55 (dd, J = 16.4 and 3.9 Hz, 1H); ^{13}C NMR ($CDCl_3$) δ 13.94 (−), 22.48 (+), 23.72 (+), 31.43 (+), 40.68 (+), 52.98 (−), 101.08 (−), 132.12 (−), 139.91 (−), 200.47 (+); HRMS calcd for $C_{11}H_{20}O_3$ 200.1413, found 200.1412.

***(E)*-4-Oxo-2-nonenal (13).** Compound **12 (**460 mg, 2.3 mmol) was added to 30 mL of 2 N HCl/acetone (1:2 v/v) with stirring for 4 h. Then, the reaction mixture was concentrated and extracted with CH_2Cl_2 (3 × 10 mL). The combined organic layer was dried (Na_2SO_4) and concentrated to afford 350 mg (100%) of **13**.^{1}H NMR ($CDCl_3$) δ 0.89 (t, J = 6.7 Hz, 3H), 1.27−1.36 (m, 4H), 1.60−1.70 (m, 2H), 2.68 (t, J = 7.4 Hz, 2H), 6.76 (dd, J = 16.5 and 6.5 Hz, 1H), 6.87 (d, J = 16.2 Hz, 1H), 9.77 (t, J = 6.7 Hz, 1H); ^{13}C NMR ($CDCl_3$) δ 13.89 (−), 22.43 (+), 23.37 (+), 31.26 (+), 41.21 (+), 137.33 (−), 144.96 (−), 193.45 (−), 200.17 (+); HRMS calcd for $C_9H_{14}O_2$ 154.0994, found 154.0995.

Preparation of 1a from 13. A solution of 29.5 mg of propylamine (0.5 mmol) in 10 mL of water was neutralized to pH 7.5 with NaH_2PO_4. To this amine solution were added $CuSO_4$ (1 mg, 0.004 mmol), 2,2′-bipyridine (1.9 mg, 0.012 mmol), and then 15.4 mg (0.1 mmol) of **13**. After 16 h, the reaction mixture was concentrated to give a brown residue, which was dissolved in 1 mL of MeOH. This crude sample was then subjected to semipreparative HPLC to afford 10 mg (39.4%) of **1a**. The NMR, mass, and fluorescence spectra of this fluorophore were identical with those for the compound isolated from the incubation of HNE with propylamine.

(*E*)-4-Oxo-2-pentenal (14). Compound **14** was prepared by a modification of the literature procedure.[45] 2-Methylfuran (18 mL, 0.2 mol), anhydrous Na_2CO_3 (42.4 g, 0.4 mol), and methanol (100 mL) were added into a three-neck round-bottomed flask. The reaction mixture was cooled to −10 °C, and a solution of 11.2 mL of bromine (0.22 mol) in 60 mL of methanol was added dropwise over 1 h. The reaction mixture was stirred at −10 °C for 3 h, and then the undissolved salts were removed by filtration. The filtrate was poured into 400 mL of saturated NaCl solution and extracted with CH_2Cl_2 (4 × 60 mL). The combined CH_2Cl_2 extracts were dried over anhydrous Na_2SO_4. After removing CH_2Cl_2, the resulting yellow oil was added into 60 mL of distilled water, stirred for 6 h, and allowed to stand overnight, followed by extraction with CH_2Cl_2 (4 × 15 mL). The CH_2Cl_2 extracts were dried with Na_2SO_4, concentrated, and distilled (65−70 °C at 11 Torr) to afford 8 g (38% based on 2-methylfuran) of **14**.

Incubation of (*E*)-4-oxo-2-pentenal (14) with Primary Amines. Compound **14** (490 mg, 5 mmol) in 10 mL of acetonitrile was added to 20 mL of an aqueous solution of 50 mmol of either ethylamine (from the 70% aqueous reagent) or propylamine, which is neutralized to pH 7.4 by adding NaH_2PO_4. The solution was incubated overnight and then extracted with EtOAc (3 × 20 mL). TLC analysis showed several spots; the major nonfluorescent product from each incubation reaction was purified by flash chromatography (EtOAc as eluent). Pyrrole dimer **15a** from reaction of **14** with ethylamine: ^{1}H NMR ($CDCl_3$) δ 1.05 (t, J = 7.23 Hz, 3H), 1.30 (t, J = 7.23 Hz, 3H), 1.68 (s, 3H), 1.87 (s, 3H), 3.12 (dq, J = 14.16 and 7.10 Hz, 1H), 3.33 (dq, J = 14.10 and 7.13 Hz, 1H), 3.79 (q, J = 7.16 Hz, 2H), 6.08 (d, J = 5.73 Hz, 1H), 6.11(d, J = 2.85 Hz, 1H), 6.56 (d, J = 2.91 Hz, 1H), 6.91 (d, J = 5.67 Hz, 1H); ^{13}C NMR ($CDCl_3$) δ 9.72 (−), 13.85 (−), 16.36 (−), 24.27 (−), 34.19 (+), 41.42 (+), 66.69 (+), 106.85 (−), 114.68 (+), 117.78 (−), 123.85 (−), 125.22 (+), 153.81 (−), 170.61 (+). HRMS calcd for $C_{14}H_{20}N_2O$ 232.1577, found 232.1572. Pyrrole dimer **15b** from reaction of **14** with propylamine: ^{1}H NMR ($CDCl_3$) δ 0.81 (t, J = 7.36 Hz, 3H), 0.87 (t, J = 7.37 Hz, 3H), 1.38−1.54 (m, 2H), 1.57−1.74 (m, 2H), 1.66 (s, 3H), 1.84 (s, 3H), 2.87−3.04 (m, 1H), 3.12−3.27 (m, 1H), 3.70 (t, J = 7.28 Hz, 2H), 6.08 (d, J = 5.90 Hz, 1H), 6.08 (d, J = 2.56 Hz, 1H), 6.53 (d, J = 2.94 Hz, 1H), 6.91 (d, J = 5.82 Hz, 1H); ^{13}C NMR ($CDCl_3$) δ 9.77, 11.11, 11.64, 21.69, 24.20, 24.37, 41.40, 48.30, 66.63, 106.59, 114.48, 118.71, 123.69, 125.29, 153.74, 170.86; HRMS calcd for $C_{16}H_{24}N_2O$ 260.1890, found 260.1894.

^{15}N-Labeled *N,N′*-Propyl-2-pentyl-2-hydroxy-1,2-dihydropyrrol-3-one Propyl Iminium (^{15}N-labeled 1a). A solution of 500 mg of ^{15}N-labeled propylamine hydrochloride (5.18 mmol) in 15 mL of water was neutralized to pH 7.30 with Na_2HPO_4. $CuSO_4 \cdot 5H_2O$ (10 mg, 0.04 mmol) and 20 mg of 2,2′-bipyridine (0.13 mmol) were slowly added, and then 200 mg (1.30 mmol) of **13** in 10 mL of acetonitrile was added. After 16 h, the reaction solution was extracted with ethyl acetate/hexane (1:1 v/v), and the water layer was concentrated and subjected to HPLC isolation. The ex/em 360/430 nm fluorescent fractions were combined, concentrated, and further purified by flash chromatography (MeOH as eluent) to afford 98 mg (30%) of [^{15}N]**1a**. ^{1}H NMR (D_2O) δ 0.81 (t, J = 6.78 Hz, 3H), 0.93 (t, J = 7.41 Hz, 3H), 0.94 (t, J = 7.38 Hz, 3H), 1.23−1.29 (m, 4H), 1.61−1.70 (m, 2H), 1.71−1.80 (m, 2H), 1.80−1.92 (m, 1H), 2.06−2.17 (m, 1H), 3.35 (t, J = 6.86 Hz, 2H), 3.45 (t, J = 7.43 Hz, 2H), 5.45 (d, J = 3.42 Hz, 1/2 H), 5.47 (d, J = 3.21 Hz, 1/2 H), 8.15 (d, J = 3.40 Hz, 1/2H), 8.18 (d, J = 3.20 Hz, 1/2 H); ^{13}C NMR (D_2O) δ 10.44, 10.63, 13.13, 21.00, 21.38, 21.66, 21.88, 30.44, 35.48, 45.98 (d, $J^{13}C-^{15}N$ = 8.85 Hz), 47.13 (d, $J^{13}C-^{15}N$ = 8.60 Hz), 87.81, 95.32 (d, $J^{13}C-^{15}N$ = 8.48 Hz), 166.74 (d, $J^{13}C-^{15}N$ = 15.0 Hz), 176.87 (d, $J^{13}C-^{15}N$ = 18.6 Hz); HRMS calcd for $C_{15}H_{29}15N_2O$ 255.2222, found 255.2242.

Fluorescence Measurements for HNE- or HPE-Derived Fluorophores and Their Analogues at Different pH Values. To assess the effect of pH on HNE- or HHE-

(45) Clauson-Kaas, N.; Limbrg, F. *Acta Chem. Scand.* **1947**, *1*, 619−623.

derived fluorophores **1a**−**c** and their analogues **9a** and **10**, each sample (5 μL) was diluted with 3 mL of buffer solution. The buffers used to maintain pH were 0.1 M HCl−NaCl (pH 1.0), 100 mM sodium phosphate (pH 3.5, 5.5, 7.0, 8.5, 9.0, 10.5), and 0.01 M NaOH (pH 12.0). Within 5 min after mixing, the fluorescence intensity was determined with excitation at 360 nm and emission at 430 nm.

Effect of NMR Shift Reagent on Fluorescence of 1b. Aliquots (10 μL) of a 10 mM solution of compound **1b** in MeOH were added to cuvettes containing 2.7 mL of methanolic solutions of europium tris(6,6,7,7,8,8,8-heptafluoro-2,2-dimethyl-3,5-octanedionate) [Eu(fod)$_3$] ranging in concentration from 0.01 to 50 mM. The fluorescence intensities at 430 nm (excitation at 360 nm) relative to a value of 20 for 0.1 μM quinine in 0.1 N aqueous H_2SO_4 were 80, 72, 66, 58, 19, and 1 for [Eu(fod)$_3$] at 0, 0.01, 0.1, 1, 10, and 50 mM, respectively.

Incubation of RNase A with HNE. RNase A (3.4 mg, 0.25 μmol) was incubated in 100 μL of 100 mM pH 7.2 sodium phosphate buffer for each sample. Then, either a solution of $CuSO_4$ (0.5 mM, 100 μL), a solution of DTPA (1 mM, 100 μL), a solution of $CuSO_4$ and DTPA (0.5 mM/1 mM, 100 μL), a solution of $CuSO_4$ and DEF (0.5 mM/1 mM, 100 μL), or the same volume of distilled water was added. The reaction was initiated by adding a solution of HNE (7.5 mM) in DMSO (50 μL). After 5 h, the reaction mixtures were quenched by adding an equal volume of a standard denaturing buffer for electrophoresis (0.3 M pH 6.8 tris, 5% SDS, 5% 2-mercaptoethanol, 50% glycerol, and 0.02% bromophenol blue). Then, each sample was heated to 100 °C for 5 min and analyzed by SDS-polyacrylamide gel eletrophoresis system with 5% stacking and 30% resolving gels.[46] Proteins were stained by GelCode Blue Stain Reagent (Pierce, Rockford, IL).

Effect of Base and Borohydride on the HNE−RNase-Derived Fluorophore. RNase A (34 mg, 2.5 μmol) was incubated in a mixture consisting of 1 mL of 200 mM pH 7.2 sodium phosphate buffer, 1 mL of 0.1 mM $CuSO_4$, and 0.5 mL of a 7.5 mM solution of HNE in DMSO for 65 h with stirring and occasional exposure to air. Then, 0.5 mL of a 12% aqueous solution of SDS was added, the reaction mixture was stirred for another 10 min, and five 0.5 mL aliquots were individually added to 2.0 mL portions of 200 mM buffer solutions: one at pH 7.2 sodium phosphate, two at pH 9.0 sodium borate, and two at pH 10.0 sodium borate. Immediately, 10 mg of $NaBH_4$ was dissolved into one of the reaction mixtures at pH 9.0 and one at pH 10.0. The relative fluorescence intensity (ex/em 360/430 nm) and absorbance at 360 nm were determined immediately and after 15, 30, 60, 90, 120, 240, and 360 min. At this time, the pH values of the reaction mixtures with added $NaBH_4$ were determined to be unchanged.

Fluorescence Monitoring of the Reaction of 6-Aminocaproic Acid with HNE or HPE. To 10 mL of a 30% aqueous methanolic solution of 6-aminocaproic acid (0.1, 0.5, 1.0, or 2.5 M) and NaCl (2.4, 2.0, 1.5, and 0 M), with the ionic strength kept constant at 2.5 M, was added HNE (7.8 mg, 0.05 mmol) or HPE (6.1 mg, 0.05 mmol). The reaction mixtures were kept stirring for 144 h, during which time 100 μL aliquots were periodically removed and diluted with 3 mL of H_2O for ex/em 360/430 nm fluorescence measurement.

Isolation of Reduced Adducts 18−21 from the Reaction of HNE or HPE with Primary Amines. A solution of *n*-butylamine (2.92 g, 40 mmol) in 90 mL of water was neutralized to pH 7.8 by adding NaH_2PO_4, and a solution of 0.78 g (5 mmol) of HNE in 35 mL of acetonitrile was added. Then, $CuSO_4$ (20 mg, 0.04 mmol) and 2,2′-bipyridine (19 mg, 0.13 mmol) were slowly added. The reaction mixture was kept stirring at room temperature. The progress of reaction was monitored by spectrofluorometry (ex/em 360/430 nm) and HPLC analysis at regular intervals. After 24 h incubation, half of the reaction mixture was quenched by adding 0.47 g (150 mmol) of $NaBH_4$. The remaining half portion was quenched 5 d later (144 h). For each reduction, the excess $NaBH_4$ was decomposed by adding 20 mL of acetone after 5 min. Then, the organic solvents (acetonitrile and acetone) in the reaction mixture were removed under reduced pressure, and the aqueous residue was extracted with CH_2Cl_2 (3 × 10 mL). The combined extracts were dried over Na_2SO_4 and concentrated to afford a yellow residue which was analyzed by ^{1}H NMR and then subjected to preparative TLC separation (4:1 CH_2Cl_2-MeOH as eluent) to afford the reduced 1:1 adduct **3-(butylamino)-1,4-nonanediol** (**18**) and the reduced 2:1 adduct **1,3-bis(butylamino)-4-nonanol** (**19**). **18**: ^{1}H NMR ($CDCl_3$) δ 0.92 (m, 6H), 1.30−1.67 (m, 14H), 2.60−2.93 (m, 3H), 3.72−3.95 (m, 3H); ^{13}C NMR ($CDCl_3$) δ 13.97 (−), 14.05 (−), 20.46 (+), 22.63 (+), 26.10 (+), 28.94 (+), 31.92 (+), 32.53 (+), 33.99 (+), 46.71 (+), 62.30 (+), 62.77 (−), 70.15 (−); HRMS cacld for $C_{13}H_{30}NO_2$ $(M + H)^+$ 232.2277 found 232.2270. **19**: ^{1}H NMR ($CDCl_3$) δ 0.92 (t, 9H), 1.27−1.73 (m, 18H), 2.49−2.78 (m, 7H, CH_2N and CHN), 3.61 (m, 1H); ^{13}C NMR ($CDCL_3$) δ 14.00 (−), 20.46 (+), 22.68 (+), 26.16 (+), 27.93 (+), 31.84 (+), 32.08 (+), 32.29 (+), 34.11 (+), 46.17 (+), 47.08 (+), 49.34 (+), 61.69 (−), 70.46 (−); HRMS calcd for $C_{17}H_{39}N_2O$ $(M + H)^+$ 287.3062, found 287.3010. The ratio of the two adducts present in the crude reaction mixture following reductive quench was determined from the ^{1}H NMR spectrum by integrating the unique 1H signal at 3.61 δ for **19** relative to the unique 3H region (δ 3.72−3.95) for **18**, both signals arising from the protons next to oxygen. The total yield was determined by summing the isolated yields of the two individual adducts following preparative TLC separation of a measured aliquot of the reaction mixture. The ratio of reduced 1:1 and 2:1 adducts based on the TLC-isolated material was within 10% of that indicated by ^{1}H NMR, but the percent yields in Table 1 represent the ^{1}H NMR data.

In a similar way, a reaction of ethylamine (40 mmol, 2.4 g of 70% aqueous solution) with HPE (500 mg, 5 mmol) was carried out and analyzed, yielding the reduced 1:1 adduct **3-(ethylamino)-1,4-pentanediol** (**20**) and the reduced 2:1 adduct **1,3-bis(ethylamino)-4-nonanol** (**21**). **20**: ^{1}H NMR ($CDCl_3$) δ 1.08−1.28 (m, 6H), 1.60−1.69 (m, 2H), 2.54−2.85 (m, 3H), 3.70−3.82 (m, 2H), 3.93−4.02 (m, 1H); ^{13}C NMR ($CDCl_3$) δ 15.64 (−), 19.60 (−), 29.23 (+), 41.24 (+), 61.98 (+), 63.10 (−), 66.14 (−); HRMS calcd for $C_7H_{18}NO_2$ $(M + H)^+$ 148.1338, found 148.1338. **21**: ^{1}H NMR ($CDCl_3$) δ 1.05−1.20 (m, 9H), 1.45−1.80 (m, 2H), 2.45−2.75 (m, 7H), 3.61 and 3.75 (2m, 1H total); ^{13}C NMR ($CDCl_3$) δ 15.59 (−), 15.71 (−), 19.80 (−), 31.39 (+), 42.04 (+), 43.91 (+), 45.86 (+), 62.39 (−), 68.35 (−); HRMS calcd for $C_9H_{23}N_2O$ $(M + H)^+$ 175.1810, found 175.1814. The ratio of 1:1 and 2:1 products needed for calculation of % yields in this case relied on the unique 1H multiplet at δ 3.90 for **20** and the unique signal at δ 3.61 for **21**, which represents 50% of the tertiary *H*-CO (integration of the spectrum for the isolated compound indicated a 1:1 mixture of diastereomers).

***N*-(2-Methoxyethyl)-2-pentylpyrrole (23a) and *N*-(2-Methoxyethyl)-2-ethylpyrrole (23b).** 2-Methoxyethylamine (0.23 g, 3 mmol) was added to a solution of 0.39 g of 4-oxononanal (2.5 mmol) or 0.29 g of 4-oxohexanal (2.5 mmol) in 10 mL of CH_2Cl_2. The reaction solution was kept stirring for 6 h, the CH_2Cl_2 was evaporated, and the crude residue was purified by flash chromatography with 2:1 hexanes/EtOAc to afford pure pyrroles. **23a**: yield 390 mg (80%); ^{1}H NMR ($CDCl_3$) δ 0.90 (t, J = 6.75 Hz, 3H), 1.33−1.38 (m, 4H), 1.57−1.68 (m, 2H), 2.52 (t, J = 7.76 Hz, 2H), 3.31 (s, 3H), 3.58 (t, J = 6.02 Hz, 2H), 3.96 (t, J = 6.02 Hz, 2H), 5.86 (m, 1H), 6.06 (m, 1H), 6.61 (m, 1H); ^{13}C NMR ($CDCl_3$) δ 14.08 (−), 22.58 (+), 26.21 (+), 28.64 (+), 31.79 (+), 46.05 (+), 72.52 (+), 105.30 (−), 106.95 (−), 120.17 (−), 133.48 (+); HRMS calcd for $C_{12}H_{21}NO$ 195.1624, found 195.1629. **23b**: yield 286 mg (75%); ^{1}H NMR ($CDCl_3$) δ 1.26 (t, J = 7.49 Hz, 3H), 2.57 (q, J = 7.46 Hz, 2H), 3.32 (s, 3H), 3.59 (t, J = 5.91 Hz, 3.97 (t, J = 5.85 Hz, 2H), 5.89 (m, 1H), 6.08 (m, 1H), 6.63 (m, 1H); ^{13}C NMR ($CDCl_3$) δ 12.98 (−), 19.41 (+), 46.05 (+), 59.06 (−), 72.49 (+), 104.60 (−), 106.98 (−), 120.34 (−), 134.86 (+); HRMS calcd for $C_9H_{15}NO$ 153.1155, found 153.1151.

Quantitative HPLC Analysis of HNE- or HHE-Derived Advanced Products. We investigated the role of Cu(II) on

(46) Schagger, H.; vonJagow, G. *Anal. Biochem*. **1987**, *166*, 368−379.

the formation of HNE- or HHE-derived advanced end products, namely, the corresponding 2-alkylpyrrole (**23a** or **23b**) and ex/em 360/430 nm fluorophore. A solution (1.5 mL) of HNE (30 mM) or HHE (30 mM) in acetonitrile was added to 1.5 mL of an aqueous solution of 300 mM 2-methoxyethylamine adjusted to pH 7.5, 8.5, or 9.5 by addition of NaH_2PO_4 and containing either no copper or 15 mM $(2,2'\text{-bipyridine})_2CuCl_2$. For pyrrole and fluorophore analysis, the mixtures were kept stirring at room temperature for 144 h. Then, 20 μL of reaction solution was evaluated by analytical reverse-phase HPLC and monitored by the absorbance at either 230−280 nm (for pyrrole analysis) or 355−365 nm (for fluorophore analysis). The above synthetic pyrrole samples **23a** and **23b** served as internal standards, with quantitative analysis based on peak height.

Acknowledgment. We are grateful to the National Institutes of Health for support of this work through grants HL-53315 and AG-14249.

Supporting Information Available: ^1H and ^{13}C NMR spectra of **1a**, **5**, **6**, **7**, **8**, **9a**, **10**, **12**, **13**, **15a**, **18**, **19**, **20**, **21**, **23a**, and **23b**, and ^1H-^1H COSY spectrum for **1a**. This material is available free of charge via the Internet at http://pubs.acs.org.

JO982523J